

Possibilities for inclusive diffraction at the Electron Ion Collider

Anna Staśto
Penn State University

collaboration with Nestor Armesto, Paul Newman and Wojciech Słomiński



Outline

- **Simulations of $F_L^{D(3)}$ for EIC**
 - Motivation: why is $F_L^{D(3)}$ interesting ?
 - H1 measurement
 - Proton tagging as a method for diffraction at EIC
 - Pseudodata simulation, energy beam scenarios
 - Extraction by linear fit. Kinematic range and precision
 - $F_L^{D(3)}$ and $R^{D(3)}$ ratio of longitudinal to transverse cross section
- **4D diffractive cross section and Reggeon extraction at EIC**
 - EIC pseudodata for 4D diffractive cross section with t dependence
 - Extraction of Pomeron and Reggeon partonic structure, estimate of uncertainties

Series of works on diffraction at ep/eA machines:

Inclusive diffraction in future electron-proton and electron-ion colliders

e-Print: [1901.09076](#)

Diffractive longitudinal structure function at Electron Ion Collider

e-Print: [2112.06839](#)

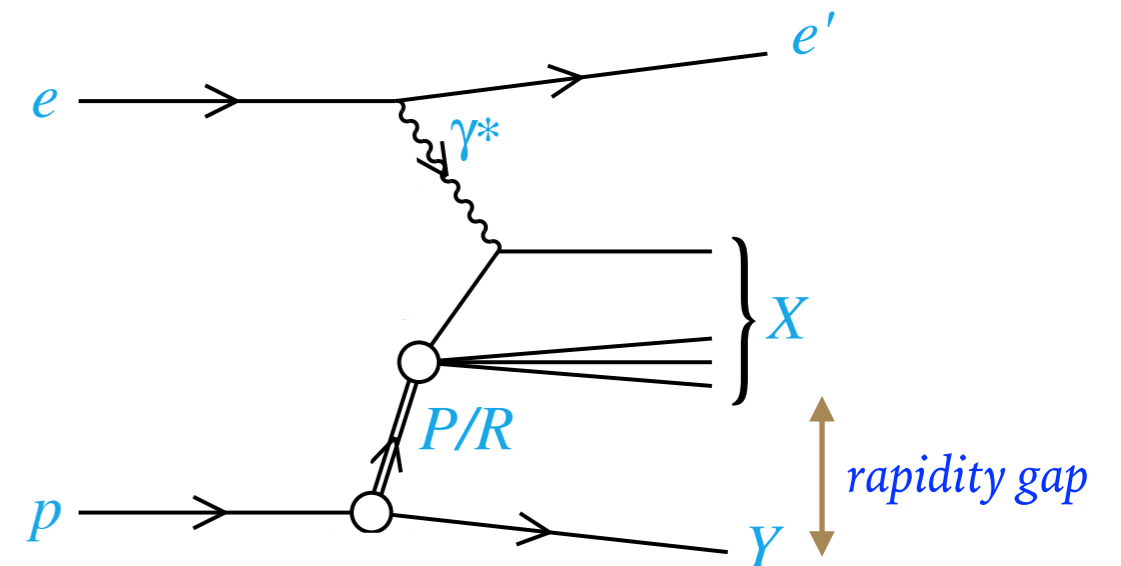
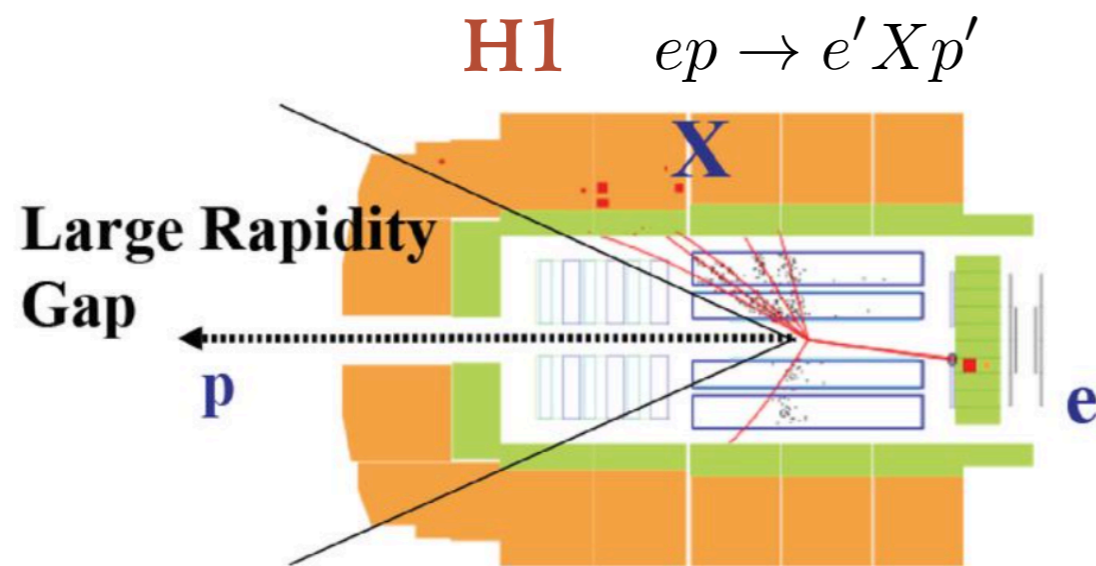
Extracting the partonic structure of colorless exchanges at Electron Ion Collider

e-Print: to appear soon

also EIC Yellow Report, Sec. 7.1.6, 8.5.7

Diffraction in DIS

- Diffractive characterized by the **rapidity gap**: no activity in part of the detector
- At HERA in electron-proton collisions: about 10% events diffractive
- Interpretation of diffraction : need **colorless exchange**

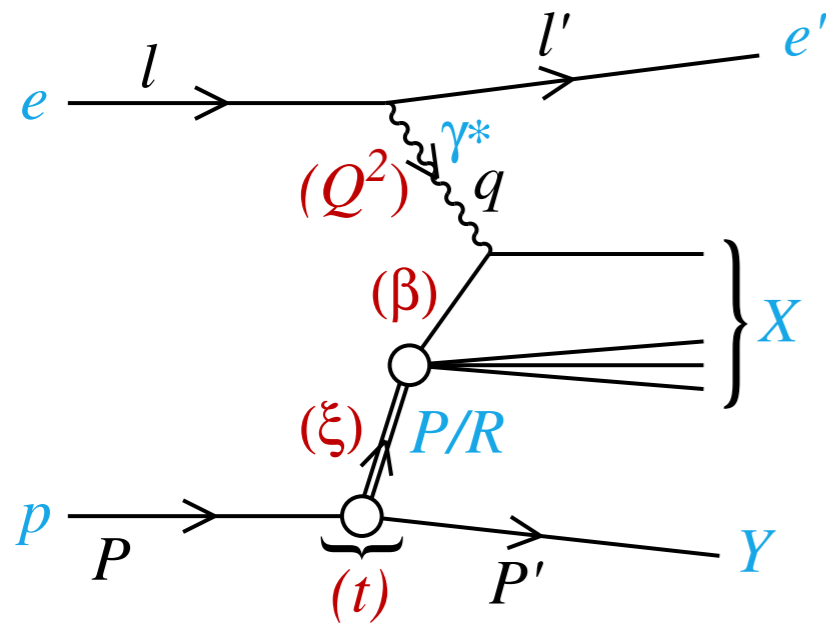


Questions:

- What is the nature of this exchange ? Partonic composition ?
- One, two, or more exchanges ? Pomeron IP , Reggeon IR ?
- Evolution ? Relation to saturation, higher twists ?
- Energy, momentum transfer dependence ?

Diffractive kinematics in DIS

Standard DIS variables:



electron-proton
cms energy squared:

$$s = (l + P)^2$$

photon-proton
cms energy squared:

$$W^2 = (q + P)^2$$

inelasticity

$$y = \frac{P \cdot q}{P \cdot l}$$

Bjorken x

$$x = \frac{Q^2}{2P \cdot q} = \frac{Q^2}{ys} = \frac{Q^2}{Q^2 + W^2}$$

(minus) photon virtuality

$$Q^2 = -q^2$$

$$x = \xi \beta$$

Diffractive DIS variables:

$$\xi = x_{IP} = \frac{x}{\beta} = \frac{Q^2 + M_X^2 - t}{Q^2 + W^2}$$

momentum fraction of the
Pomeron w.r.t hadron

$$\beta = \frac{Q^2}{2(P - P') \cdot q} = \frac{Q^2}{Q^2 + M_X^2 - t}$$

momentum fraction of parton
w.r.t Pomeron

$$t = (P' - P)^2$$

4-momentum transfer squared

Diffractive cross section, structure functions

Diffractive cross section depends on **4 variables** (ξ, β, Q^2, t):

$$\frac{d^4\sigma^D}{d\xi d\beta dQ^2 dt} = \frac{2\pi\alpha_{\text{em}}^2}{\beta Q^4} Y_+ \sigma_r^{\text{D}(4)}(\xi, \beta, Q^2, t)$$

where $Y_+ = 1 + (1 - y)^2$

Reduced cross section depends on two **structure functions**:

$$\sigma_r^{\text{D}(4)}(\xi, \beta, Q^2, t) = F_2^{\text{D}(4)}(\xi, \beta, Q^2, t) - \frac{y^2}{Y_+} F_L^{\text{D}(4)}(\xi, \beta, Q^2, t)$$

Upon integration over t :

$$F_{2,L}^{\text{D}(3)}(\xi, \beta, Q^2) = \int_{-\infty}^0 dt F_{2,L}^{\text{D}(4)}(\xi, \beta, Q^2, t)$$

$$\sigma_r^{\text{D}(3)}(\xi, \beta, Q^2) = F_2^{\text{D}(3)}(\xi, \beta, Q^2) - \frac{y^2}{Y_+} F_L^{\text{D}(3)}(\xi, \beta, Q^2)$$

When $y \ll 1$

$$\sigma_r^{\text{D}(4,3)} \simeq F_2^{\text{D}(4,3)}$$

Dimensions:

$$[\sigma_r^{\text{D}(4)}] = \text{GeV}^{-2}$$

$$\sigma_r^{\text{D}(3)} \quad \text{Dimensionless}$$

Why $F_L^{D(3)}$ is interesting?

F_L^D vanishes in the parton model, similarly to inclusive case

Gets non-vanishing contributions in QCD

As in inclusive case, particularly sensitive to the diffractive **gluon density**

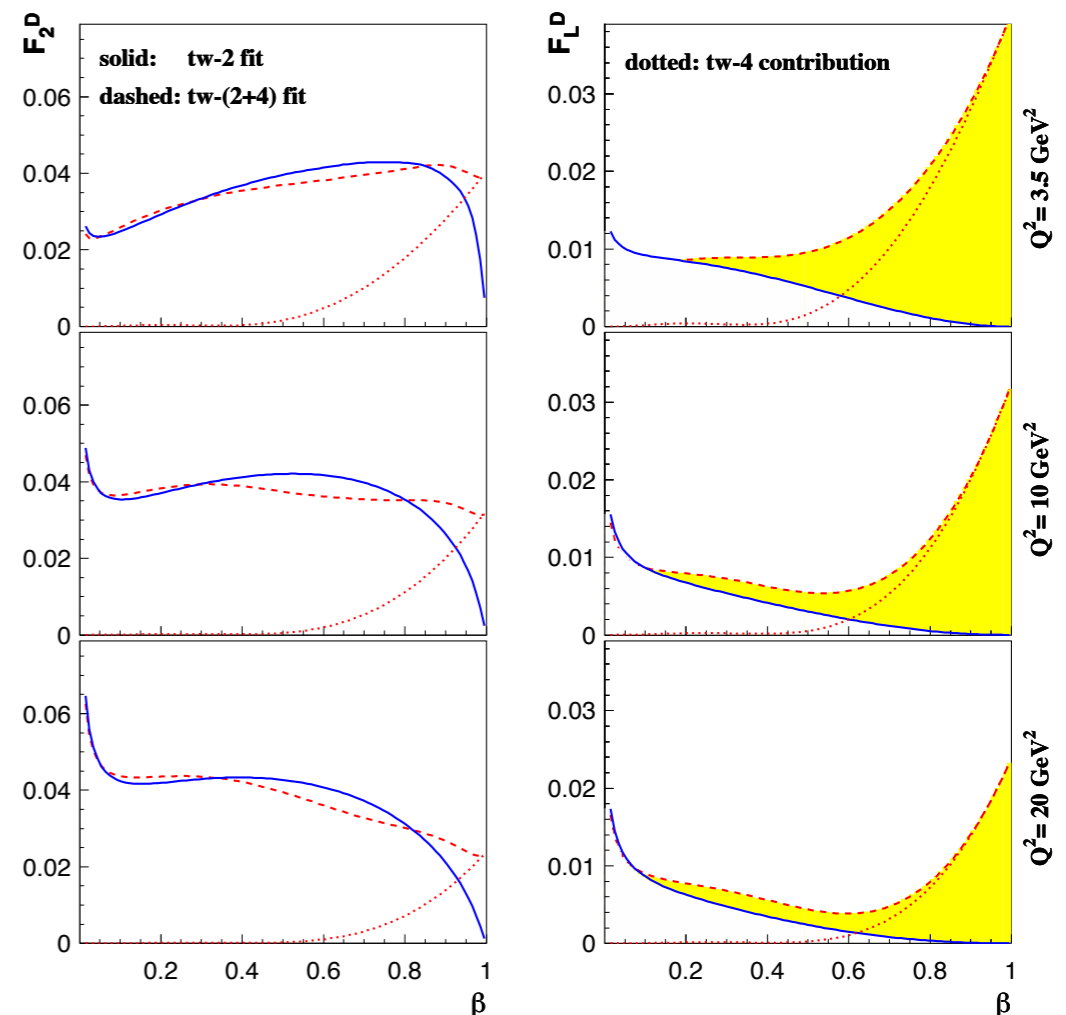
Expected large **higher twists**, provides test of the **non-linear, saturation phenomena**

Golec-Biernat, Łuszczak

Theoretical studies indicate important role of twist 4 contributions to F_L^D

F_2^D affected less by higher twists

$$x_{\mathbb{P}} \equiv \xi = 10^{-3}$$



$F_L^{D(3)}$ at HERA

Measurement requires several beam energies
 F_L^D strongest when $y \rightarrow 1$. Low electron energies

Experimentally challenging...



1107.3420[hep-ex]

H1 measurement: 4 energies, $E_p=920, 820, 575, 460$ GeV, positron beam $E_e=27.6$ GeV

E_p (GeV)	\sqrt{s} (GeV)	Q^2 range (GeV ²)	y range	Luminosity (pb ⁻¹)
460	225	$2.5 < Q^2 < 100$	$0.1 < y < 0.9$	8.5
575	252	$2.5 < Q^2 < 100$	$0.1 < y < 0.9$	5.2
920	319	$7.0 < Q^2 < 100$	$0.1 < y < 0.56$	126.8

Q^2 range	Data Set	Proton Energy E_p	Luminosity
$3 < Q^2 < 13.5$ GeV ²	1997 MB	820 GeV	2.0 pb ⁻¹
$13.5 < Q^2 < 105$ GeV ²	1997 all	820 GeV	10.6 pb ⁻¹

$$M_Y < 1.6 \text{ GeV}, |t| < 1.0 \text{ GeV}^2$$

Large errors, limited by statistics at HERA

Careful evaluation of systematics. Best precision 4%, with uncorrelated sources as low as 2%

$F_L^{D(3)}$ at HERA: extraction from linear fit

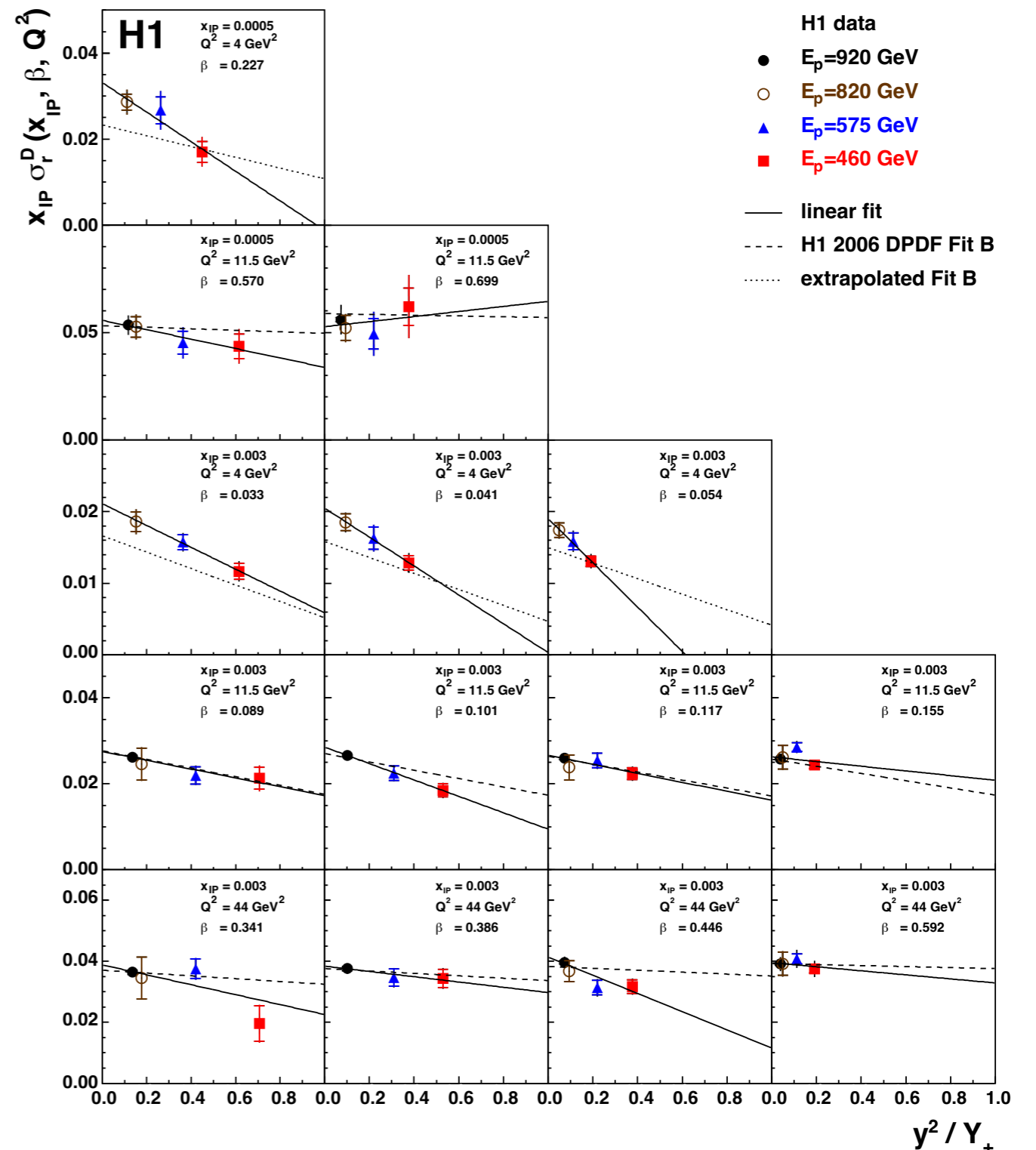
H1 analysis

$x_{IP} \sigma_r^D$ as a function of y^2/Y_+

Inner bars: statistical errors

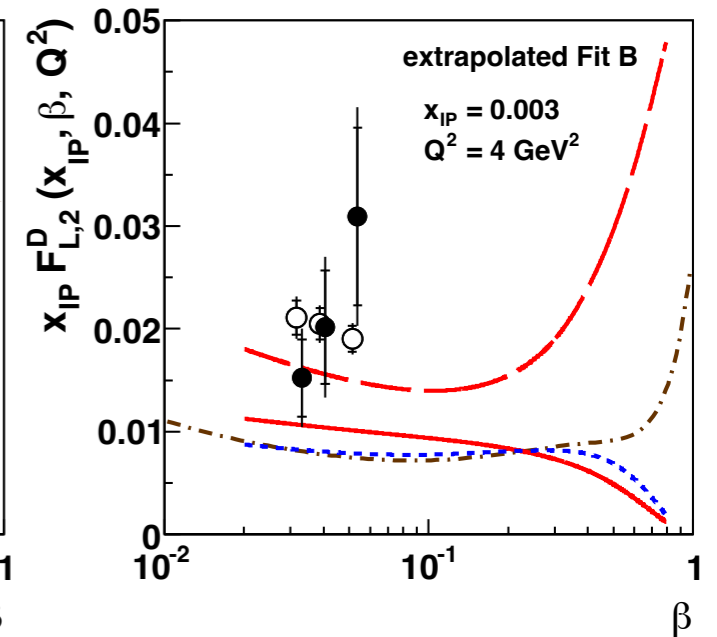
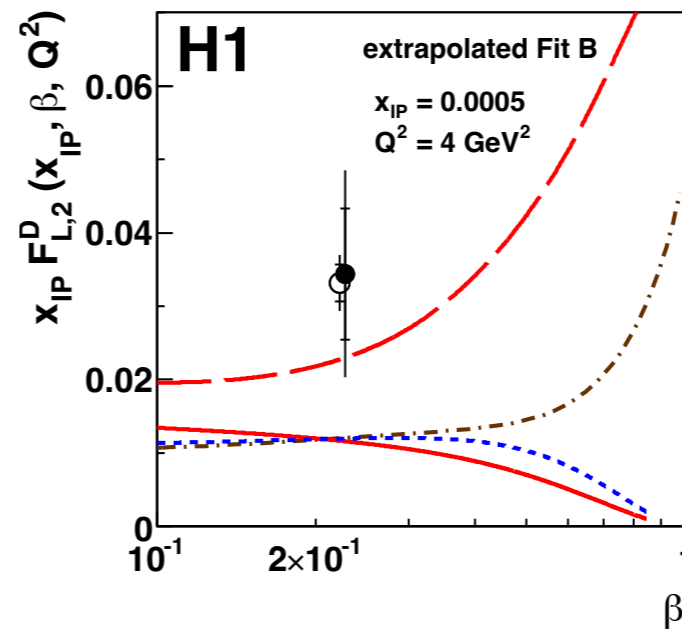
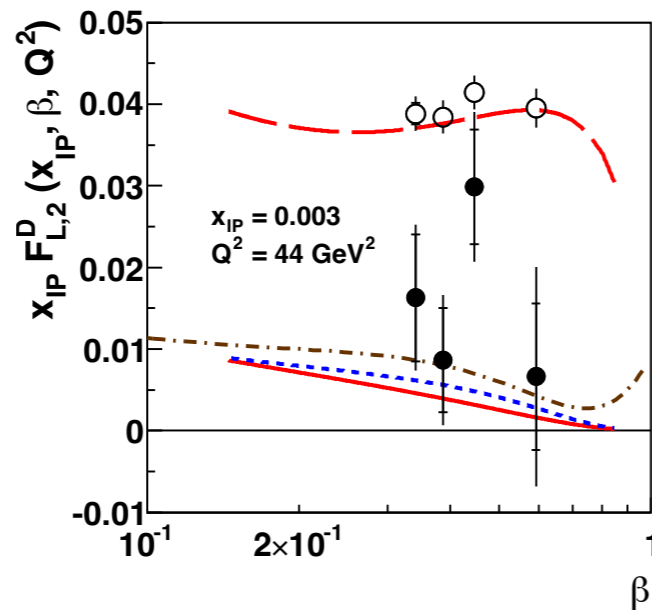
Data show linear dependence

Linear fit (solid line), the slope gives F_L^D



$F_L^D(3)$ at HERA

- $x_{IP} F_L^D$
- H1 data
- H1 2006 DPDF Fit B
- - - H1 2006 DPDF Fit A
- · - Golec-Biernat & Luszczak
- $x_{IP} F_2^D$
- H1 2006 DPDF Fit B

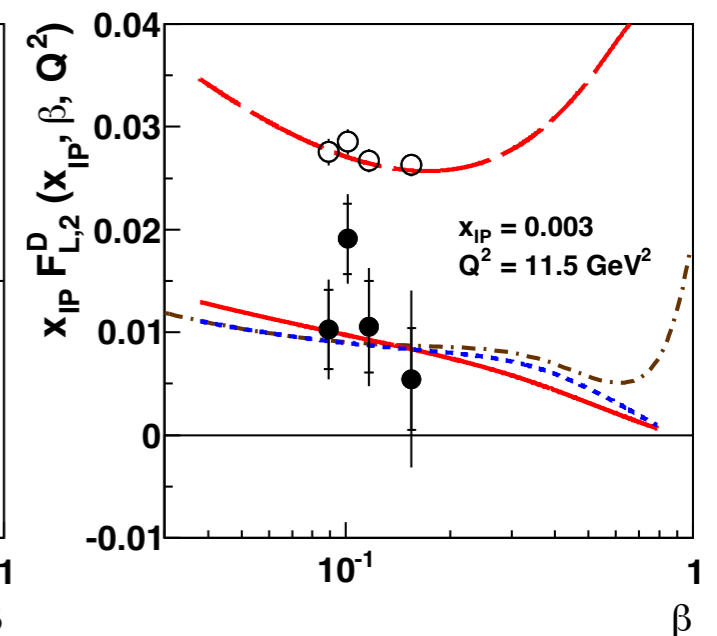
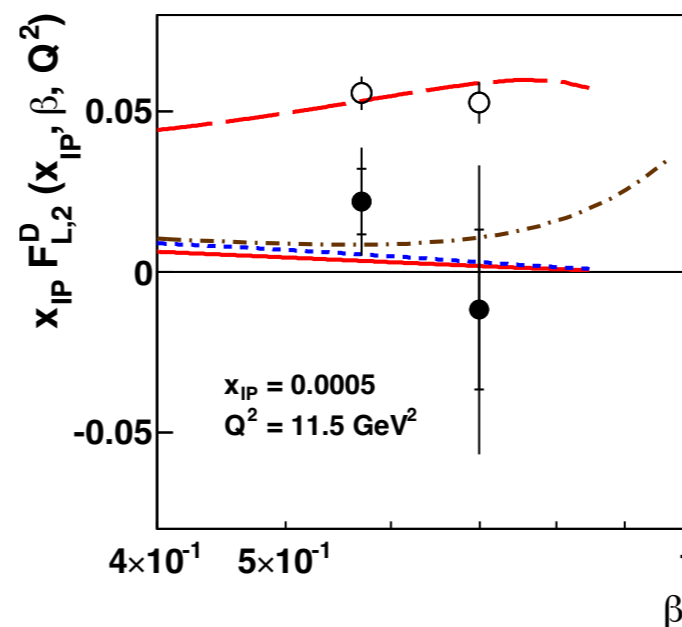


H1 conclusions:

Measurements of σ_r^D consistent with predictions from the models

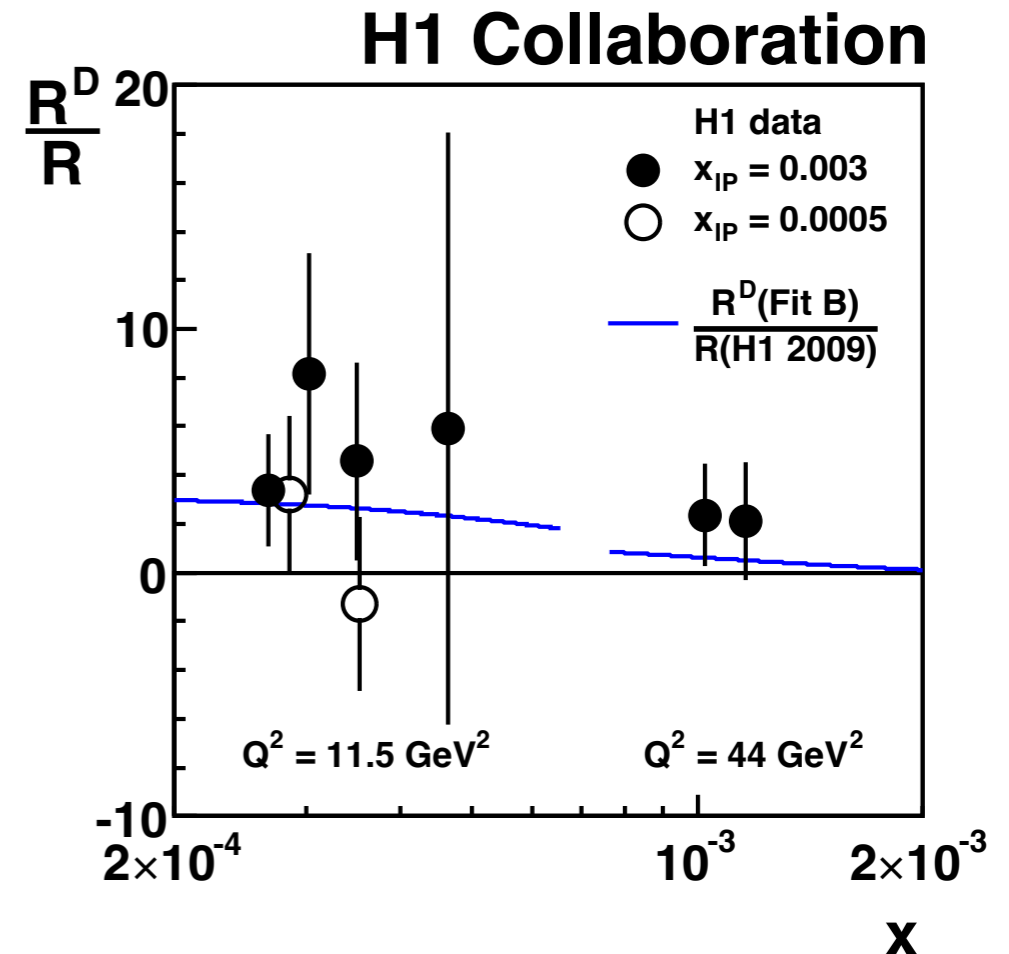
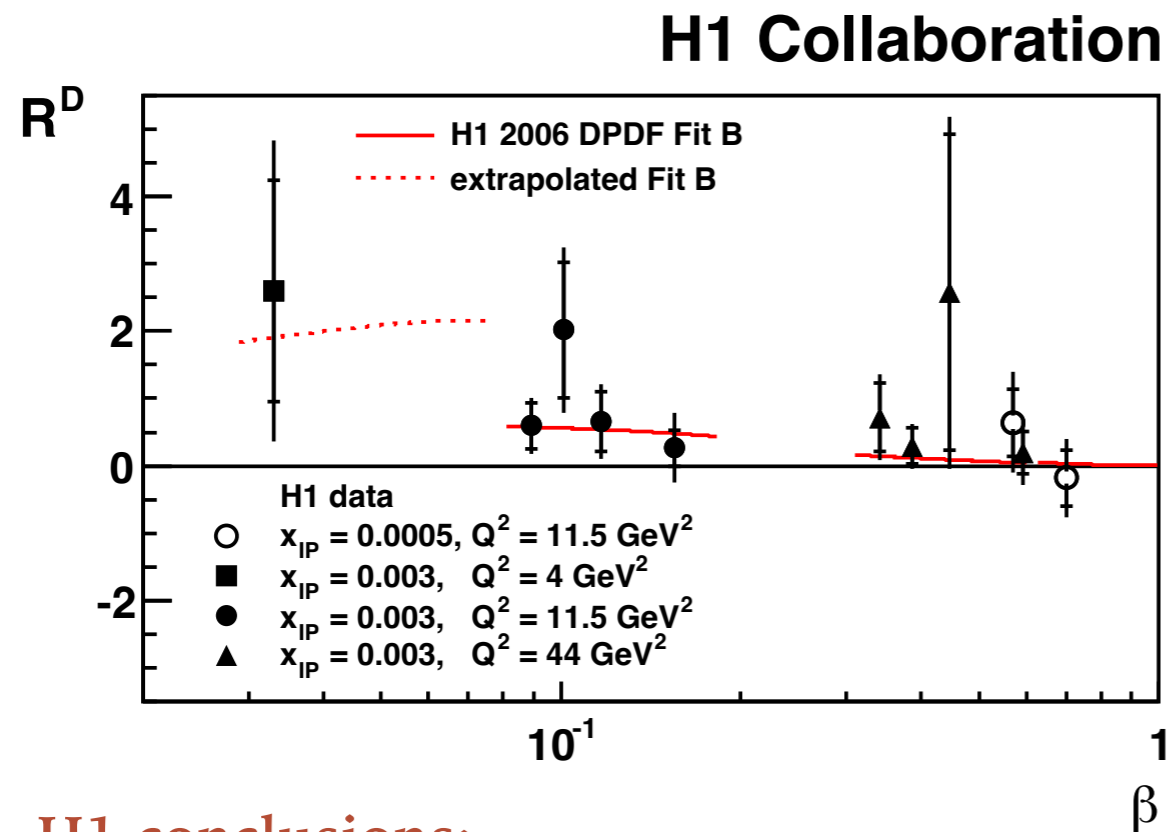
Extracted F_L^D has a tendency to be higher than the predictions, though compatible with model predictions within errors

Overall: $0 < F_L^D < F_2^D$



Diffractive ratio $R^D = F_L^D / F_T^D$ at HERA

Ratio $R^D = F_L^D / (F_2^D - F_L^D)$ longitudinal to transverse
 Ratio of ratios : diffractive R^D to inclusive R



H1 conclusions:

Data compatible with the theoretical predictions

Transverse and longitudinal polarised cross sections are of the same order of magnitude for $Q^2 = 11.5 \text{ GeV}^2$

Ratio of ratios R^D/R larger than 1, average value 2.8.

R^D/R data indicate that longitudinally polarised cross section plays a larger role in the diffractive case than in inclusive case

Phase space (x, Q^2) EIC-HERA

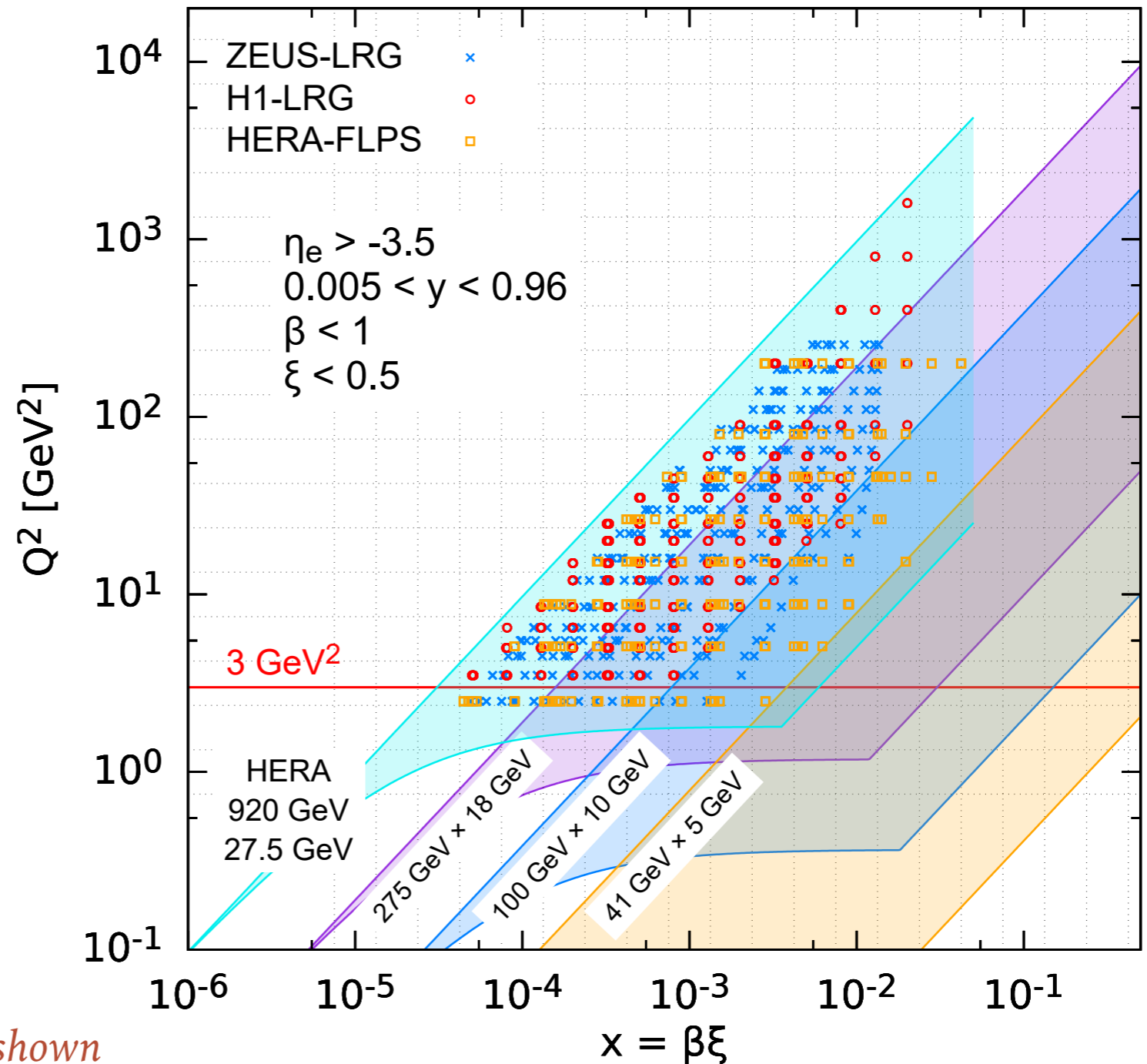
EIC can operate at various energy combinations

Can cover wide range of x

Large instantaneous luminosity

Statistics should not be a limiting factor

EIC 3 scenarios - HERA



Only selected energy scenarios at EIC shown

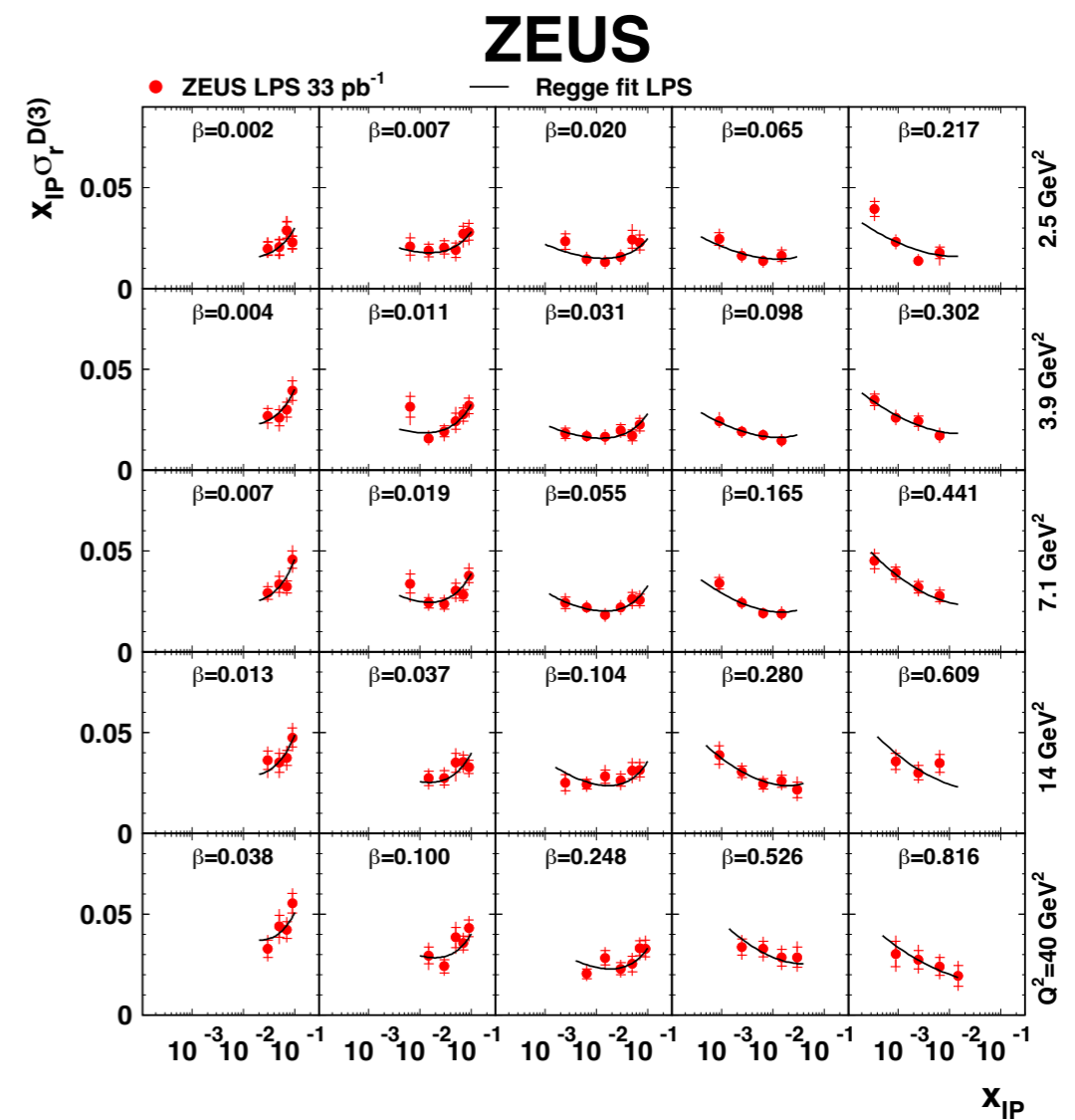
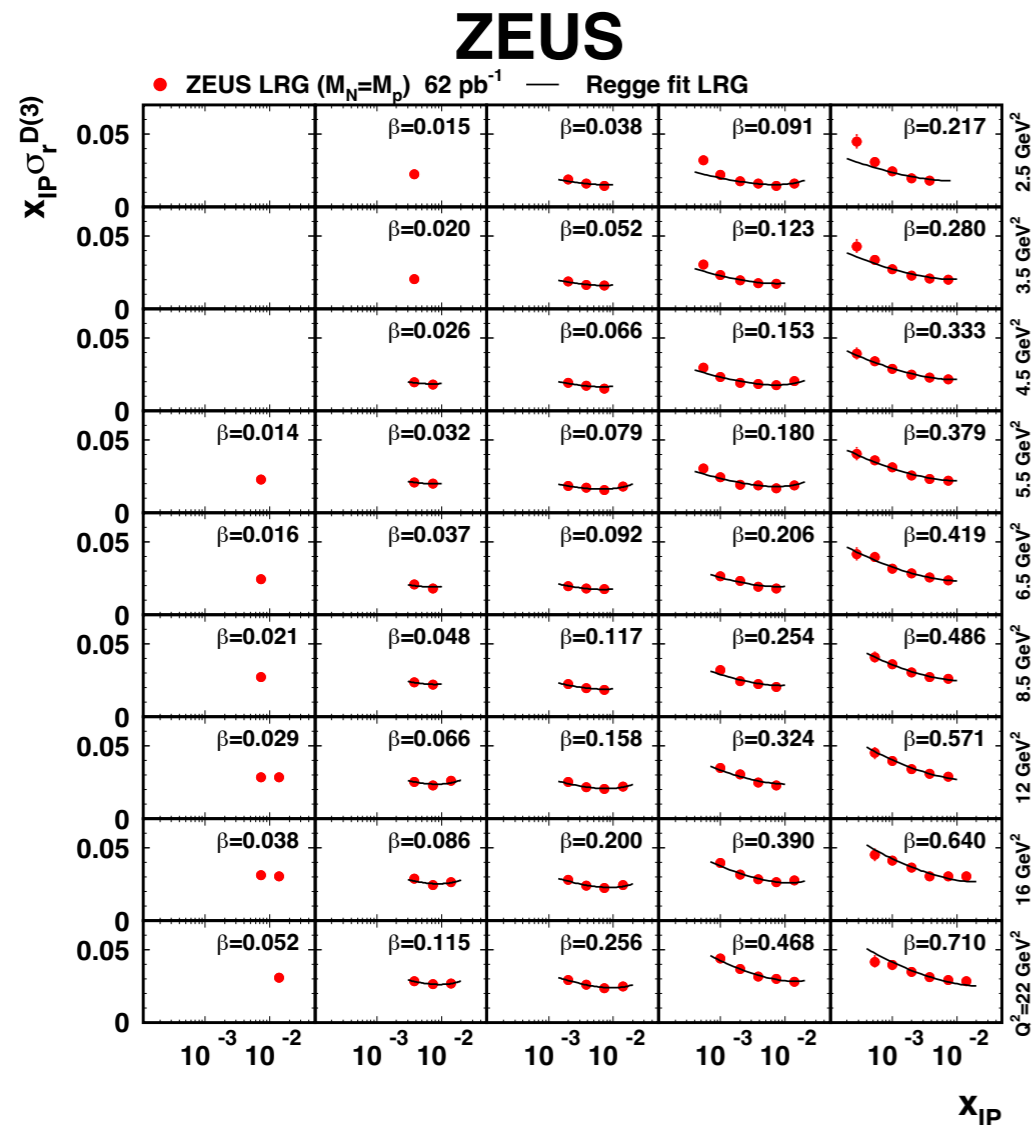
Measurement methods: LRG vs LP

Large Rapidity Gap method:

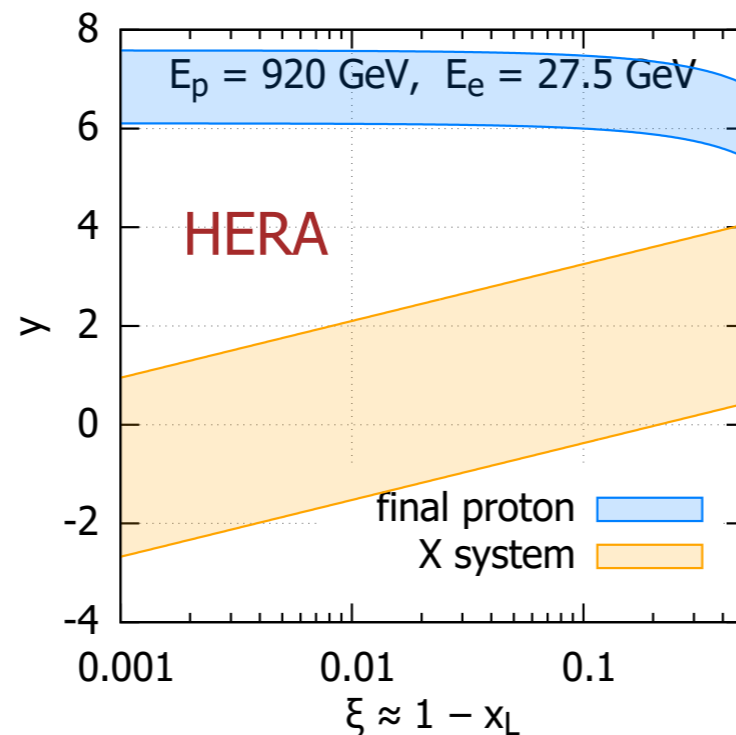
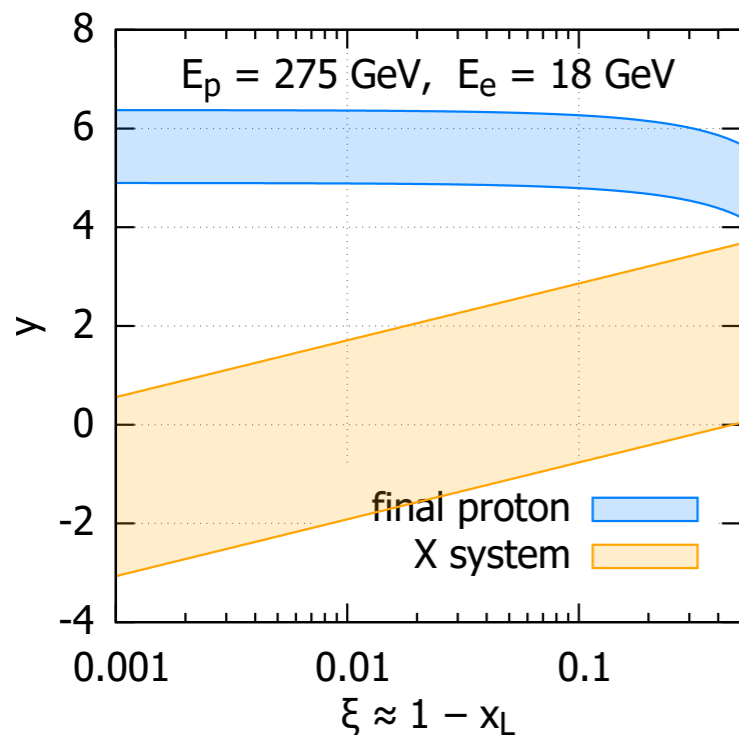
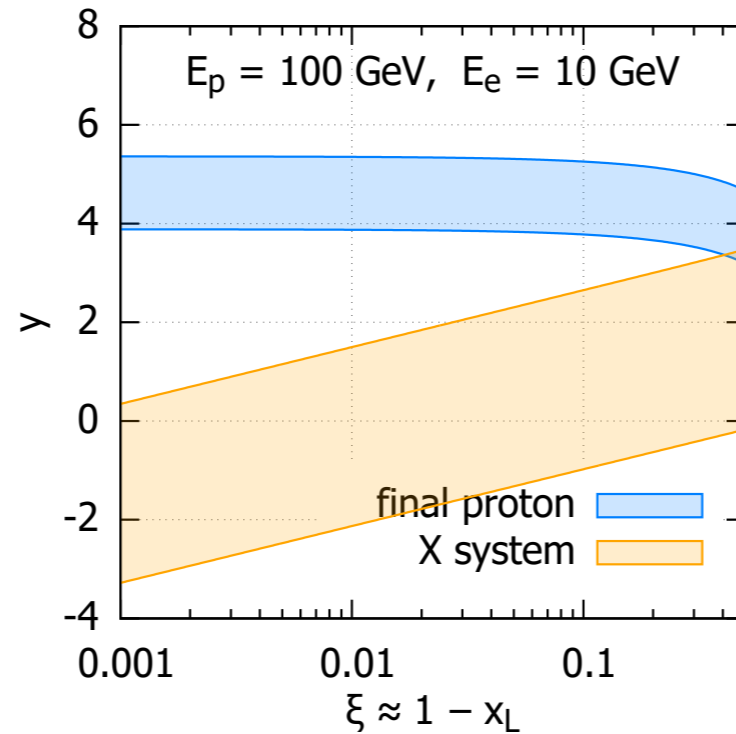
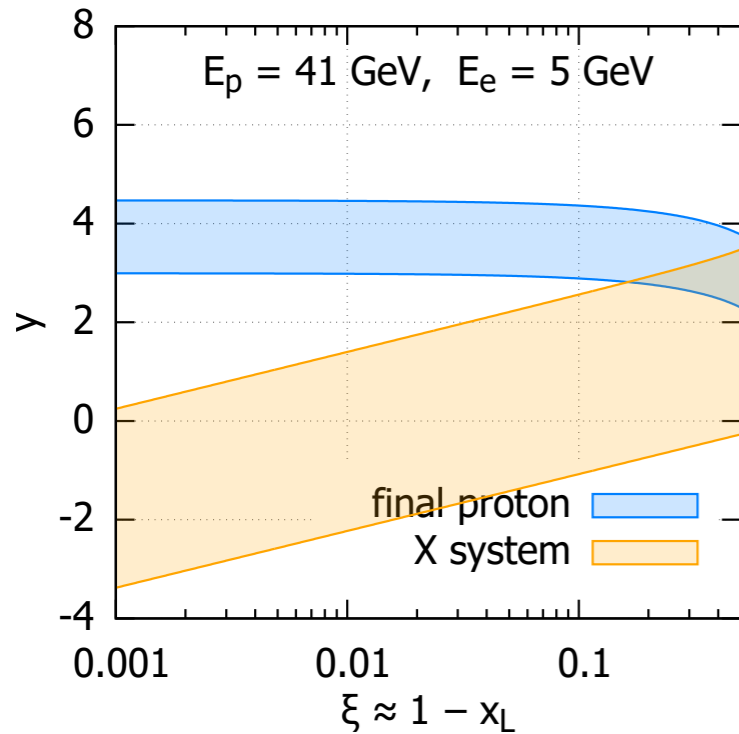
request a large rapidity gap (ex. ZEUS 2009 $\xi < 0.02$)

Proton Tagging (Leading Proton) method:

detection of a leading proton (ex. Leading Proton Spectrometer in ZEUS, Forward Proton Spectrometer in H1, can go to higher $\xi < 0.1$)



Rapidity range at EIC in diffraction



Rapidity range of proton and undecayed diffractive system X

$$p_T^{proton} < 4 \text{ GeV}$$

$$0.1 < \beta < 0.9$$

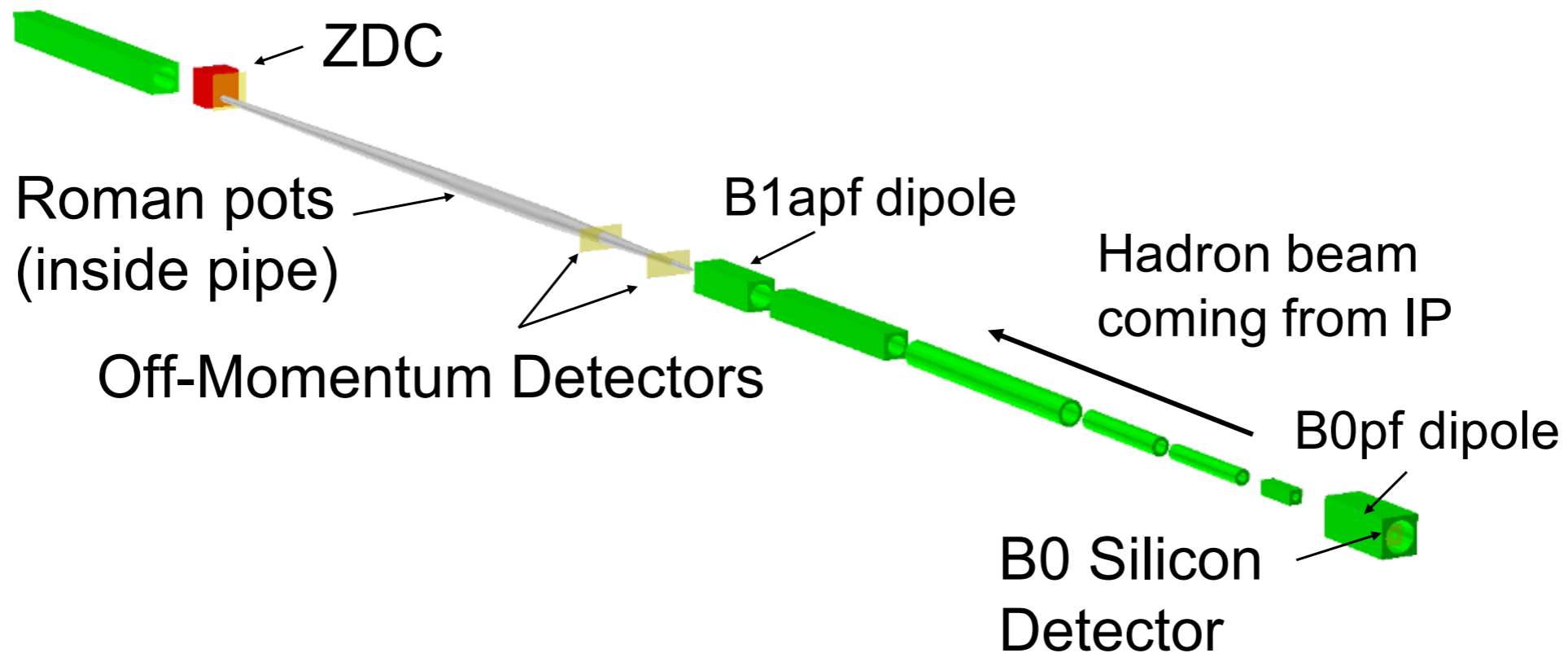
$$0.005 < y < 0.96$$

HERA: LRG method reliable for gaps > 3 units of rapidity

EIC: fairly large gaps ($\Delta\eta \geq 4$) exist for smallest ξ and largest s

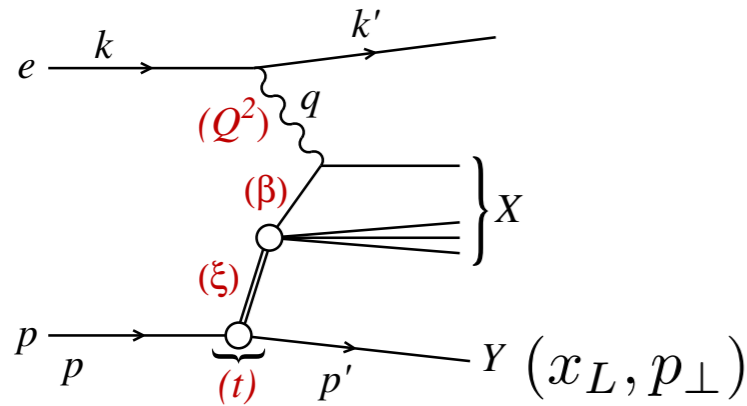
However, through most region LRG method may be challenging at EIC

Far forward detectors at EIC



Detector	Angle	Position [m]
ZDC	$\theta < 5.5$ mrad	37.5
Roman Pots	$0.5 < \theta < 5.0$ mrad	26.0, 28.0
Off-momentum detectors	$\theta < 5.0$ mrad	22.5, 25.5
B0	$6.0 < \theta < 20.0$ mrad	$5.4 < z < 6.4$

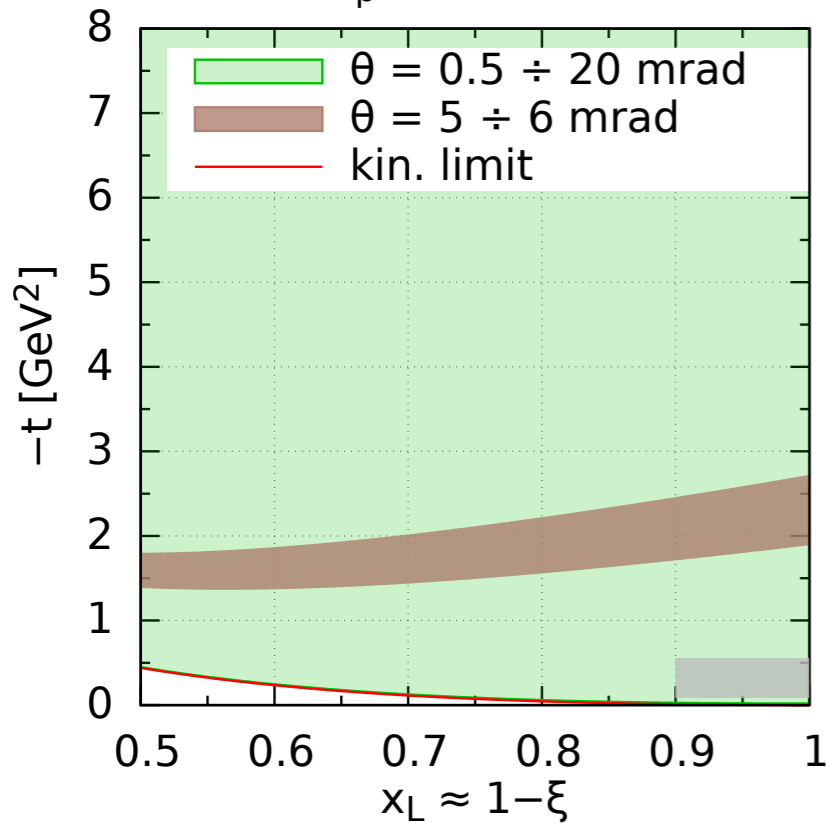
Final proton tagging



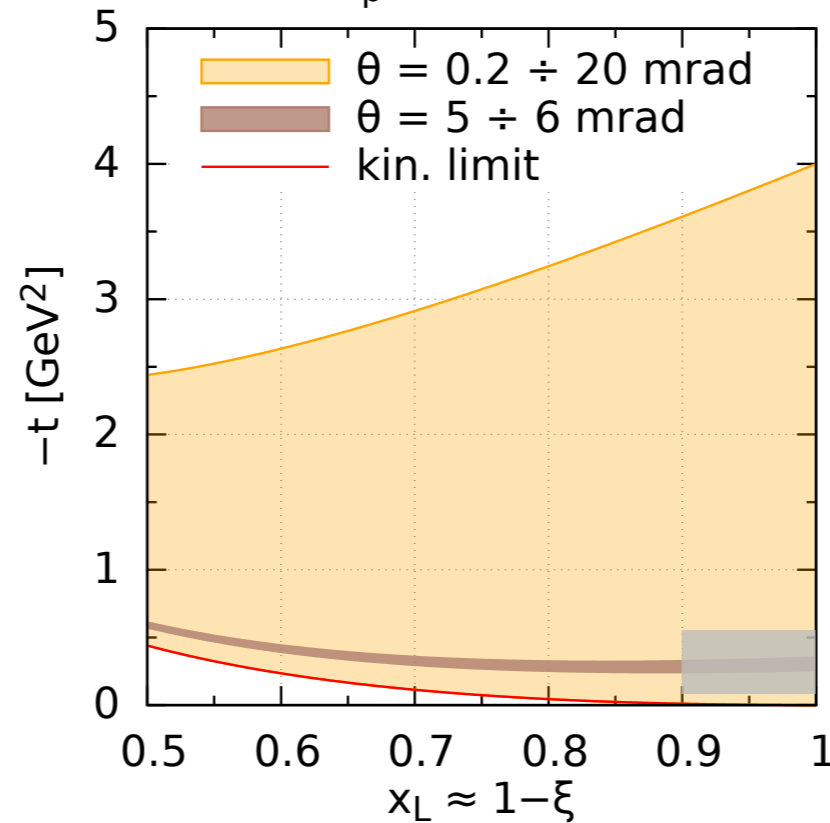
Small angle acceptance i.e. Roman pots

(x_L, p_\perp, θ) measured in LAB, collinear (e,p) frame

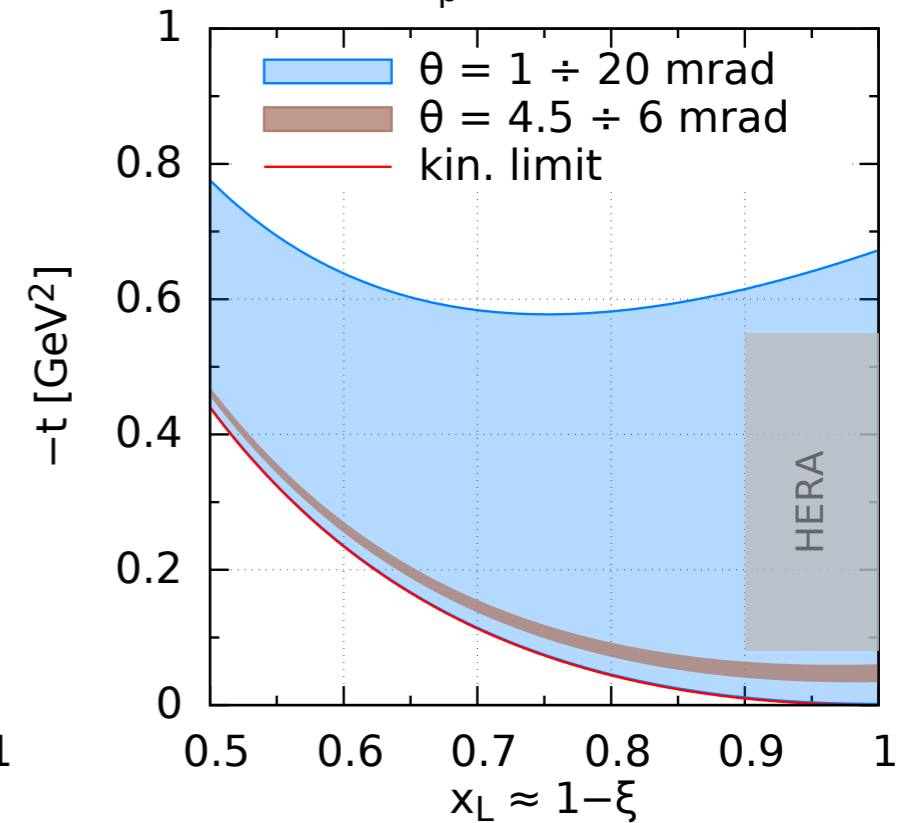
$E_p = 275$ GeV



$E_p = 100$ GeV



$E_p = 41$ GeV



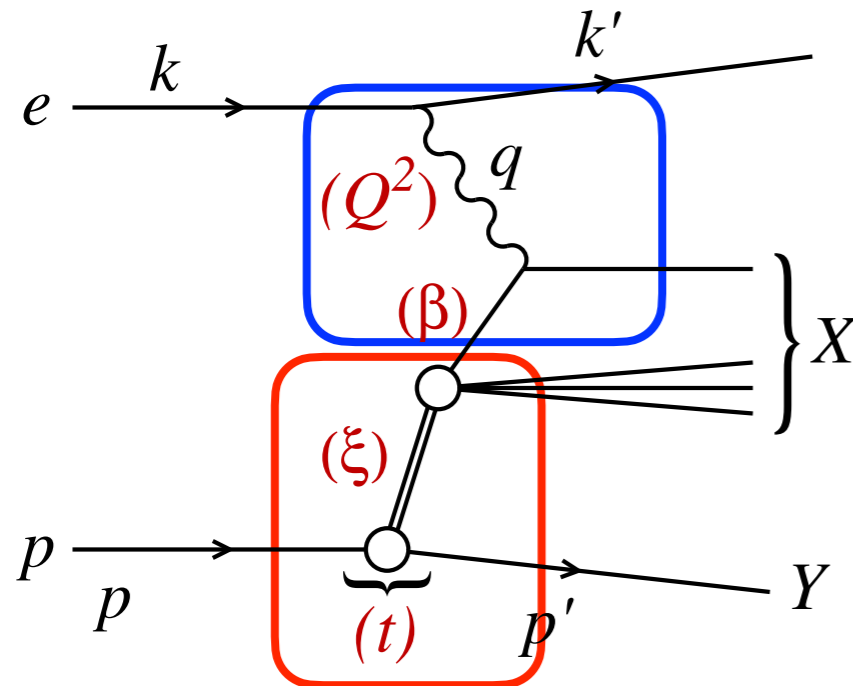
Much better than at HERA

Best way to select diffractive events through proton tagging

$$t = -\frac{p_\perp^2}{x_L} - \frac{(1-x_L)^2}{x_L} m_p^2$$

Pseudodata generation: collinear factorization for diffraction

Use the collinear factorization for the description of HERA and pseudodata simulation



Collins

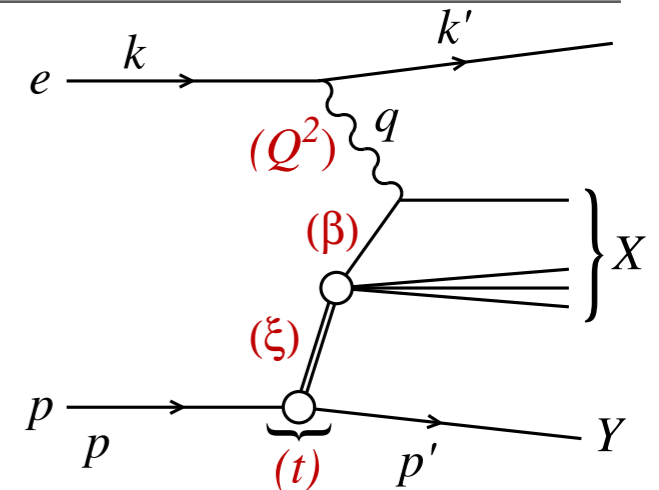
Collinear factorization in diffractive DIS

$$F_{2/L}^{D(4)}(\beta, \xi, Q^2, t) = \sum_i \int_{\beta}^1 \frac{dz}{z} C_{2/L,i} \left(\frac{\beta}{z}, Q^2 \right) f_i^D(z, \xi, Q^2, t)$$

- Diffractive cross section can be factorized into the convolution of the perturbatively calculable **partonic cross sections** and **diffractive parton distributions (DPDFs)**
- Partonic cross sections are the **same as in the inclusive DIS**
- The DPDFs are non-perturbative objects, but evolved perturbatively with **DGLAP**

Pseudodata generation: model for diffractive structure functions

- Parametrization of the DPDFs as in H1 and ZEUS analysis
- **Regge factorization** assumed
- $(\beta(\text{or } z), Q^2)$ dependence in parton distribution of diffractive exchange factorized from flux factors with (t, ξ) dependence
- Dominant term '**Pomeron**', at low ξ
- At higher ξ additional exchanges '**Reggeons**' need to be included



$$f_i^{D(4)}(z, \xi, Q^2, t) = \underbrace{f_{IP}^p(\xi, t)}_{\text{Pomeron}} f_i^{IP}(z, Q^2) + \underbrace{f_{IR}^p(\xi, t)}_{\text{Reggeon}} f_i^{IR}(z, Q^2)$$

Regge type flux:

$$f_{IP,IR}^p(\xi, t) = A_{IP,IR} \frac{e^{B_{IP,IR}t}}{\xi^{2\alpha_{IP,IR}(t)-1}}$$

Trajectory:

$$\alpha_{IP,IR}(t) = \alpha_{IP,IR}(0) + \alpha'_{IP,IR} t.$$

For t-integrated case

$$f_i^{D(3)}(z, \xi, Q^2) = \phi_{IP}^p(\xi) f_i^{IP}(z, Q^2) + \phi_{IR}^p(\xi) f_i^{IR}(z, Q^2)$$

Integrated flux:

$$\phi_{IP,IR}^p(\xi) = \int dt f_{IP,IR}^p(\xi, t)$$

Pomeron PDFs obtained via NLO DGLAP evolution starting at initial scale $\mu_0^2 = 1.8 \text{ GeV}^2$

$$z f_i(z, \mu_0^2) = A_i z^{B_i} (1-z)^{C_i} \quad i=q,g$$

Reggeon PDFs taken from the GRV fits to the pion structure function (**could also be determined at EIC!**)

Pseudodata generation: energy choice

$$\sigma_{\text{red}}^{\text{D}(3)} = F_2^{\text{D}(3)}(\beta, \xi, Q^2) - Y_L F_L^{\text{D}(3)}(\beta, \xi, Q^2) \quad \text{Integrated over t-momentum transfer}$$

$$Y_L = \frac{y^2}{Y_+} = \frac{y^2}{1 + (1 - y)^2}$$

Can disentangle $F_2^{\text{D}(3)}$ from $F_L^{\text{D}(3)}$ by varying energy and performing the linear fit in Y_L .

$$y = \frac{Q^2}{xs} = \frac{Q^2}{\beta\xi s} \quad \text{Need to vary the energy } \sqrt{s} \text{ to change } y \text{ for fixed } (\beta, \xi, Q^2)$$

EIC energies for electron and proton:

$$E_e = 5, 10, 18 \text{ GeV}$$

$$E_p = 41, 100, 120, 165, 180, 275 \text{ GeV}$$

		E_p [GeV]					
		41	100	120	165	180	275
E_e [GeV]	5	29	45	49	57	60	74
	10	40	63	69	81	85	105
	18	54	85	93	109	114	141

S-17 all 17 combinations

S-9 **9 - bold red**

S-5 **5 - green** (EIC preferred)

Pseudodata generation

Binning and cuts

Uniform logarithmic binning, 4 bins per order of magnitude in each β, Q^2, ξ

Bins in (ξ, β, Q^2) , common to at least four beam setups

$Q^2 > 3 \text{ GeV}^2$ both H1 and ZEUS fits indicate deterioration of fits for low Q^2

$0.96 > y > 0.005$ expected coverage of the experiment

Simulations

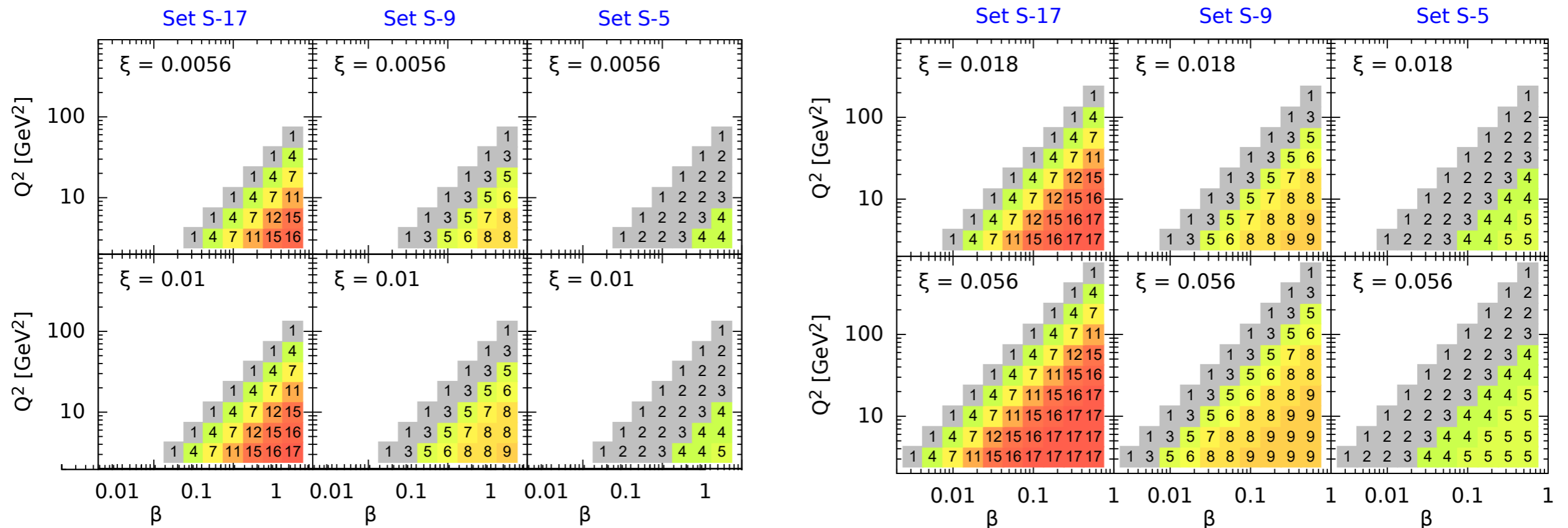
Cross section generation from ZEUS-SJ diffractive PDFs evolved with DGLAP

Assumed $\delta_{\text{sys}} = 1\text{-}2\%$, extrapolated from HERA 2% uncorrelated systematics; normalization/correlated systematics negligible effect on extraction of F_L^D

δ_{stat} from 10 fb^{-1} integrated luminosity

Several random samples are generated

Kinematic range and number of points



Count of different beam energy combinations for S-17, S-9, S-5

Only points with more than 4 combinations are taken for F_L extraction (in H1 analysis 3 points)

Set-17: 364, set-9: 285, set-5: 160 values of F_L

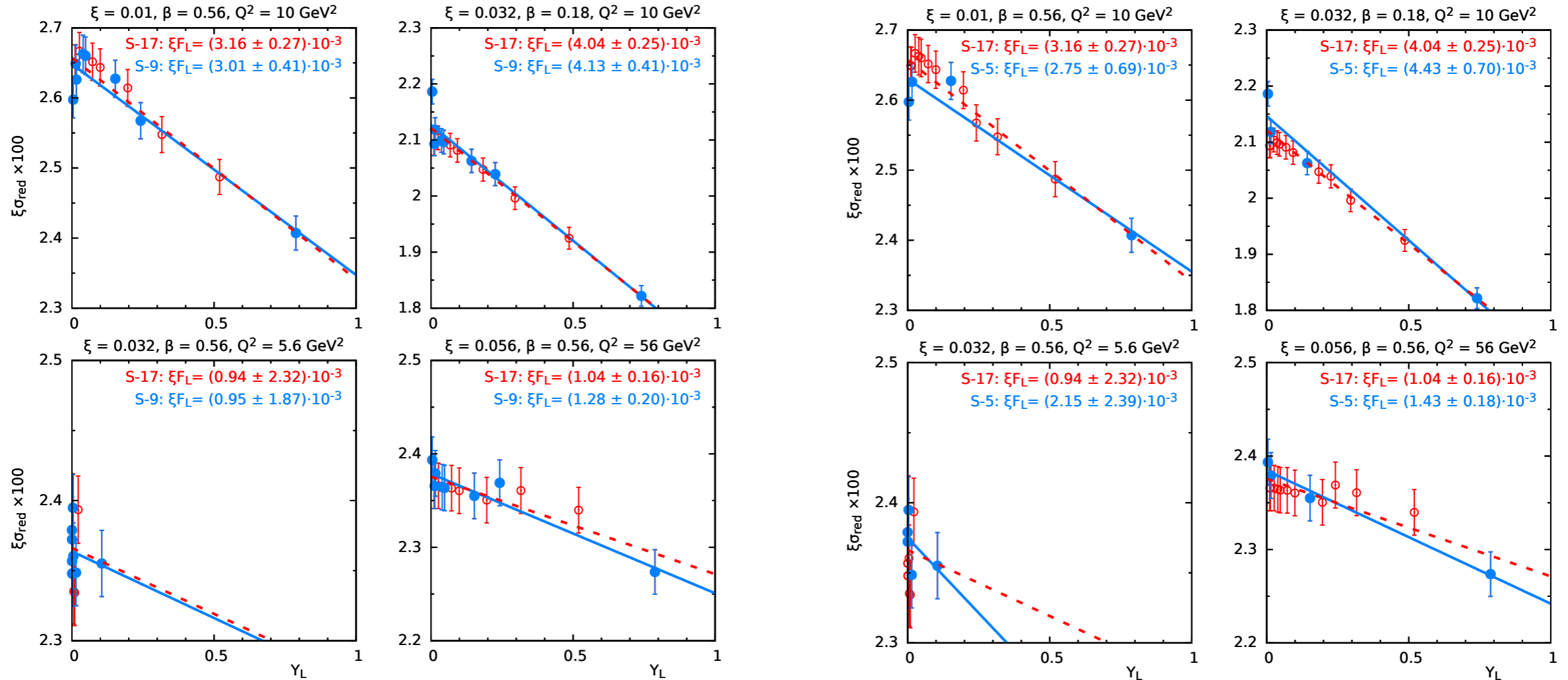
$F_L^{D(3)}$ extraction

$$\sigma_r = F_2(\xi, \beta, Q^2) - Y_L F_L(\xi, \beta, Q^2) \quad \text{as a function of } Y_L$$

Bins in (ξ, β, Q^2)

$\sigma_{\text{red}} = F_2 - Y_L F_L$ fit for $\delta_{\text{sys}} = 1\%$, CL = 68%, MC sample b, set S-9

$\sigma_{\text{red}} = F_2 - Y_L F_L$ fit for $\delta_{\text{sys}} = 1\%$, CL = 68%, MC sample b, set S-5



Uncorrelated systematics 1%

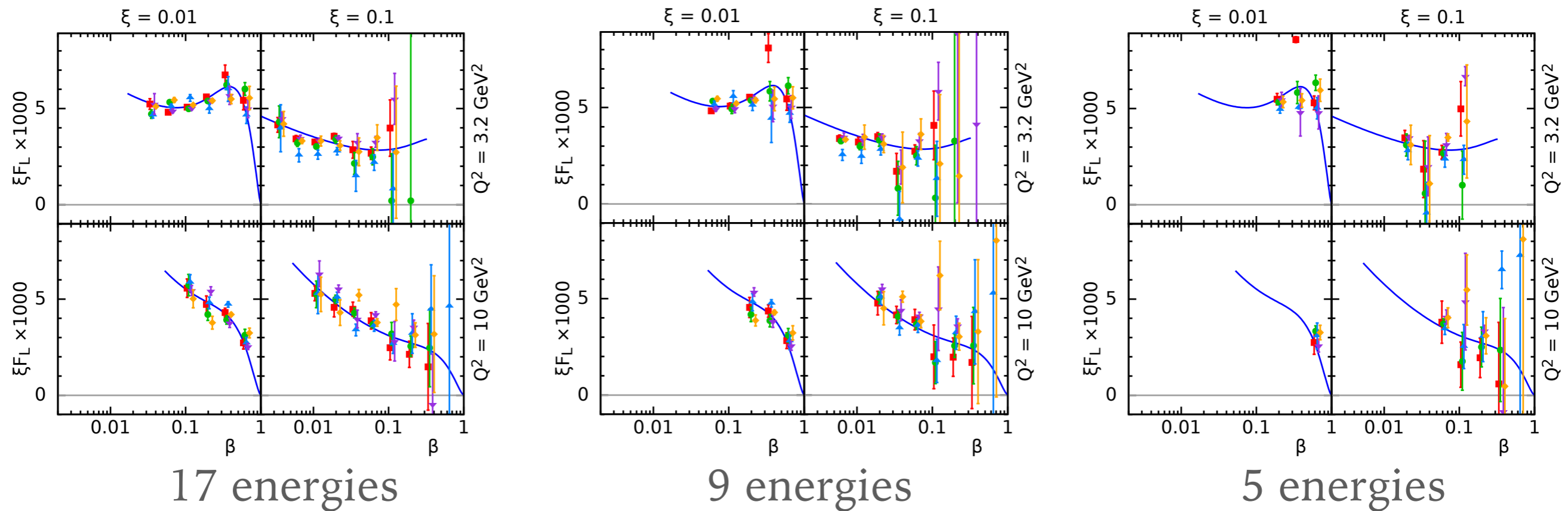
Differences between S-17 and S-9, S-5 small

Increase in error bar on the extraction when smaller number of energy points

Largest errors for bins with shortest range of Y_L

Simulated measurement of $F_L^{D(3)}$ vs β in bins of (ξ, Q^2)

Uncorr. systematic error 1%, 5 MC samples to illustrate fluctuations



Small differences between S-17 and S-9, small reduction to range and increase in uncertainties.

More pronounced reduction in range and higher uncertainties in S-5.

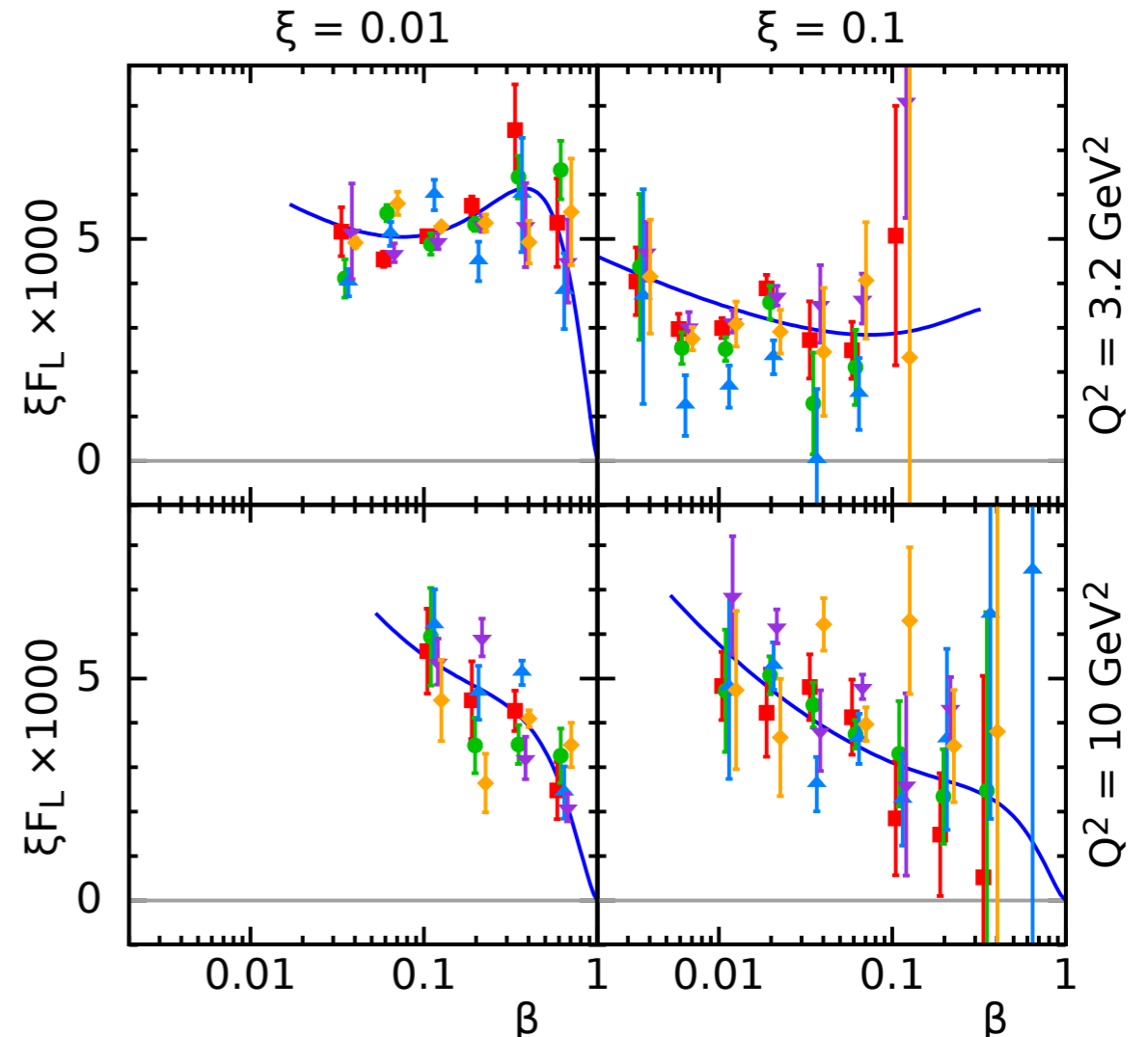
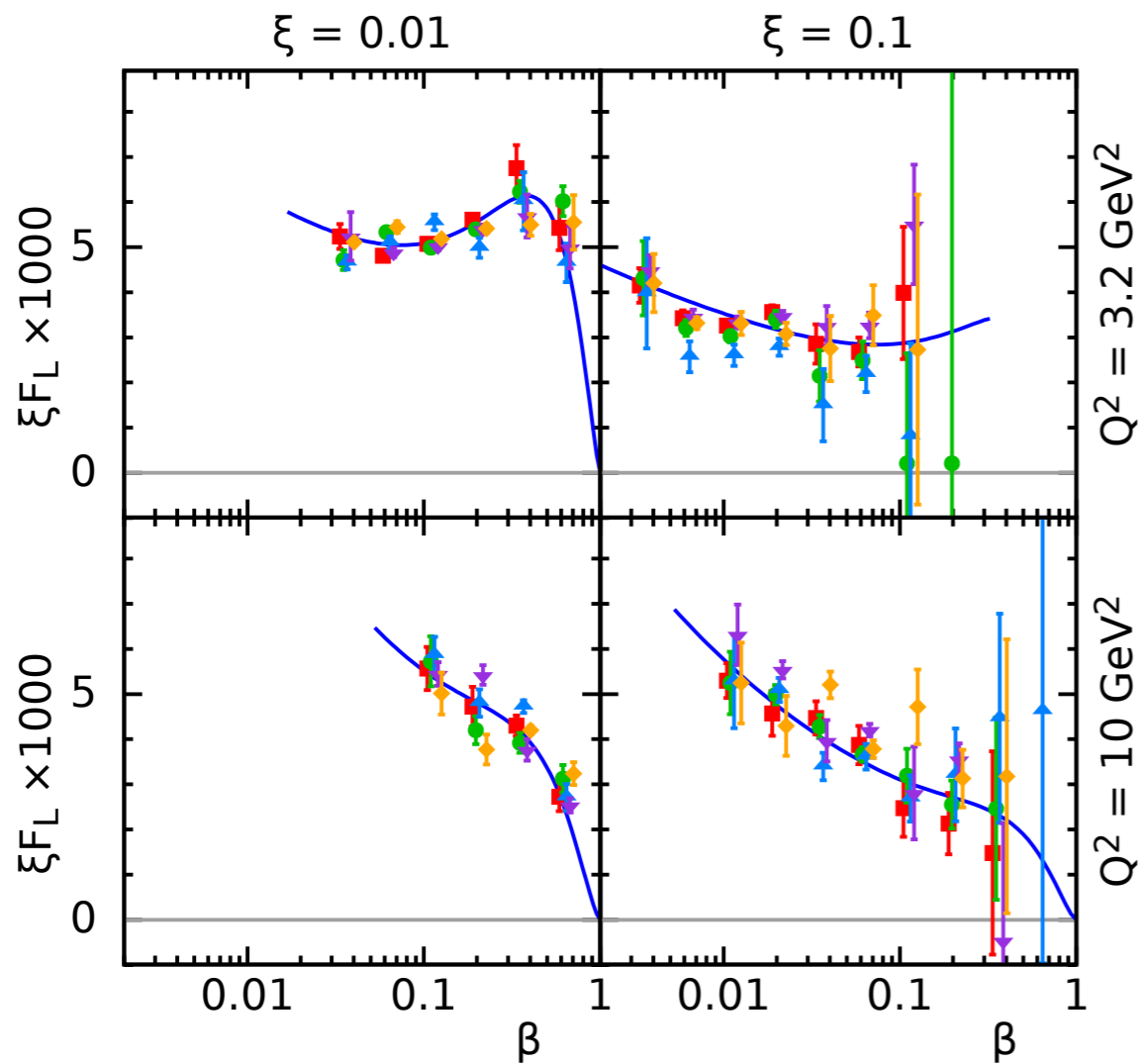
An extraction of F_L^D possible with EIC-favored set of energy combinations

Simulated measurement of $F_L^{D(3)}$ vs β in bins of (ξ, Q^2)

S-17

$\delta_{\text{sys}} = 1\%$

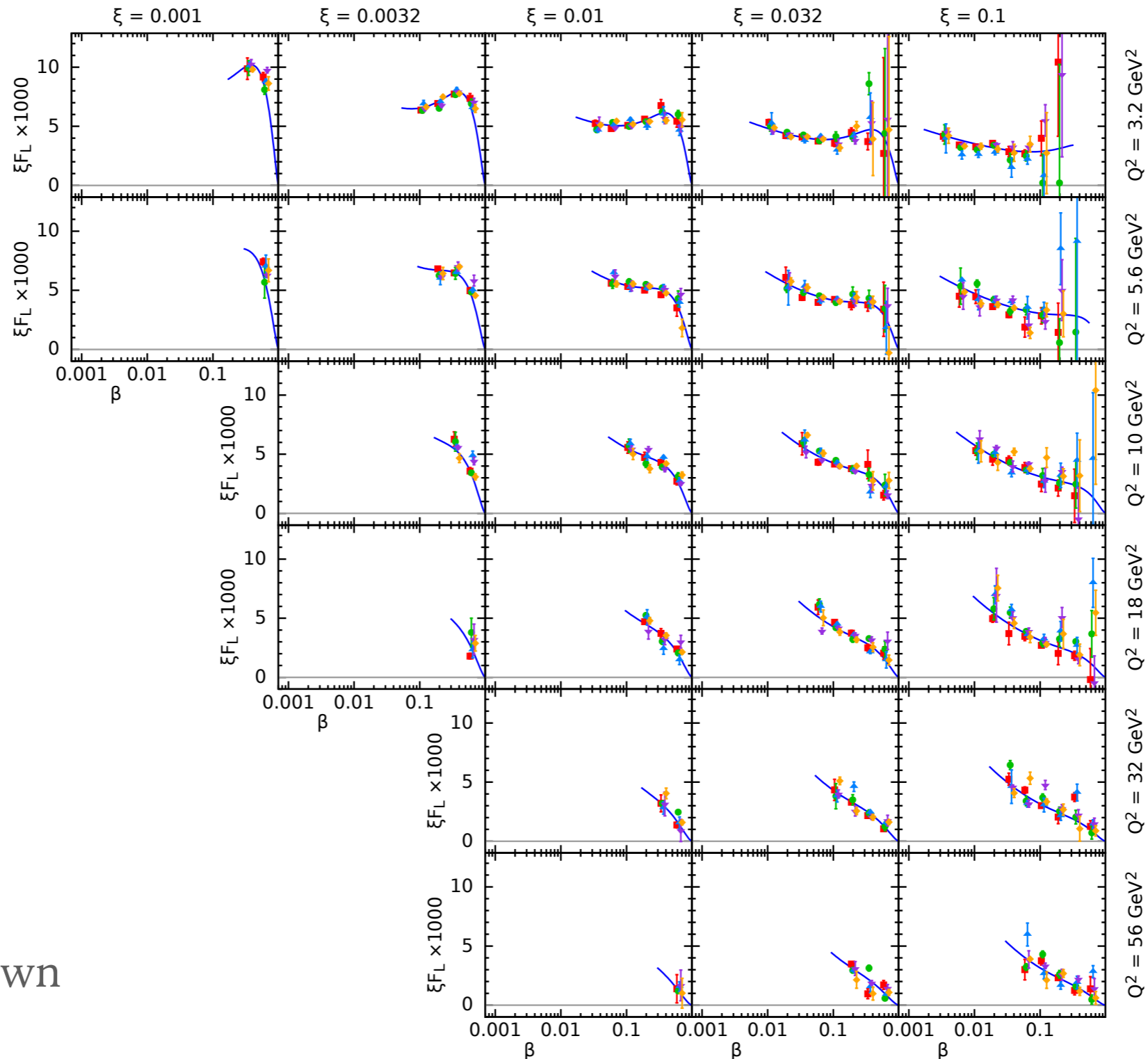
$\delta_{\text{sys}} = 2\%$



Change from 1% to 2% results in roughly twice large error bars

Statistical errors negligible

Simulated measurement of $F_L^{D(3)}$ vs β in bins of (ξ, Q^2)



S-17

$\delta_{\text{sys}} = 1\%$

more bins shown

$F_L^{D(3)}$ fit accuracy

Estimate the accuracy of extraction for $F_L^{D(3)}$

Generate several MC samples of pseudodata and perform fits

Use direct arithmetic averaging

average

$$\bar{v} = \frac{S_1}{N}$$

variance

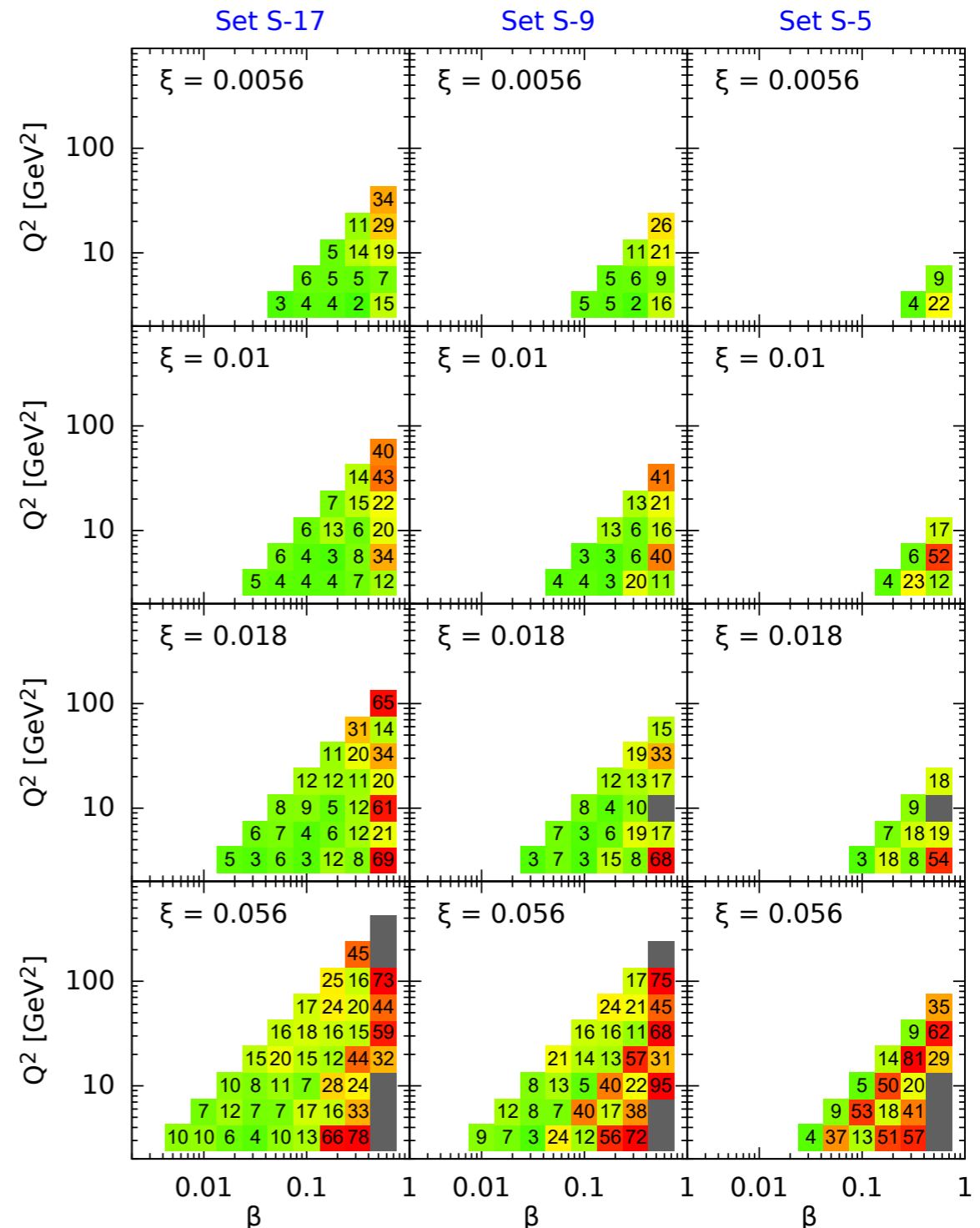
$$(\Delta v)^2 = \frac{S_2 - S_1^2/N}{N-1}$$

$$S_n = \sum_{i=1}^N v_i^n$$

where v_i is the value of F_L^D

in Monte Carlo sample i

F_L fit accuracy for $\delta_{\text{sys}} = 1\%$



$R^D = F_L^D / F_T^D$ ratio of longitudinal to transverse

Ratio of cross sections for longitudinally polarized to transverse polarized photons

$$R^{D(3)} = F_L^{D(3)} / F_T^{D(3)}$$

$$F_T^{D(3)} = F_2^{D(3)} - F_L^{D(3)}$$

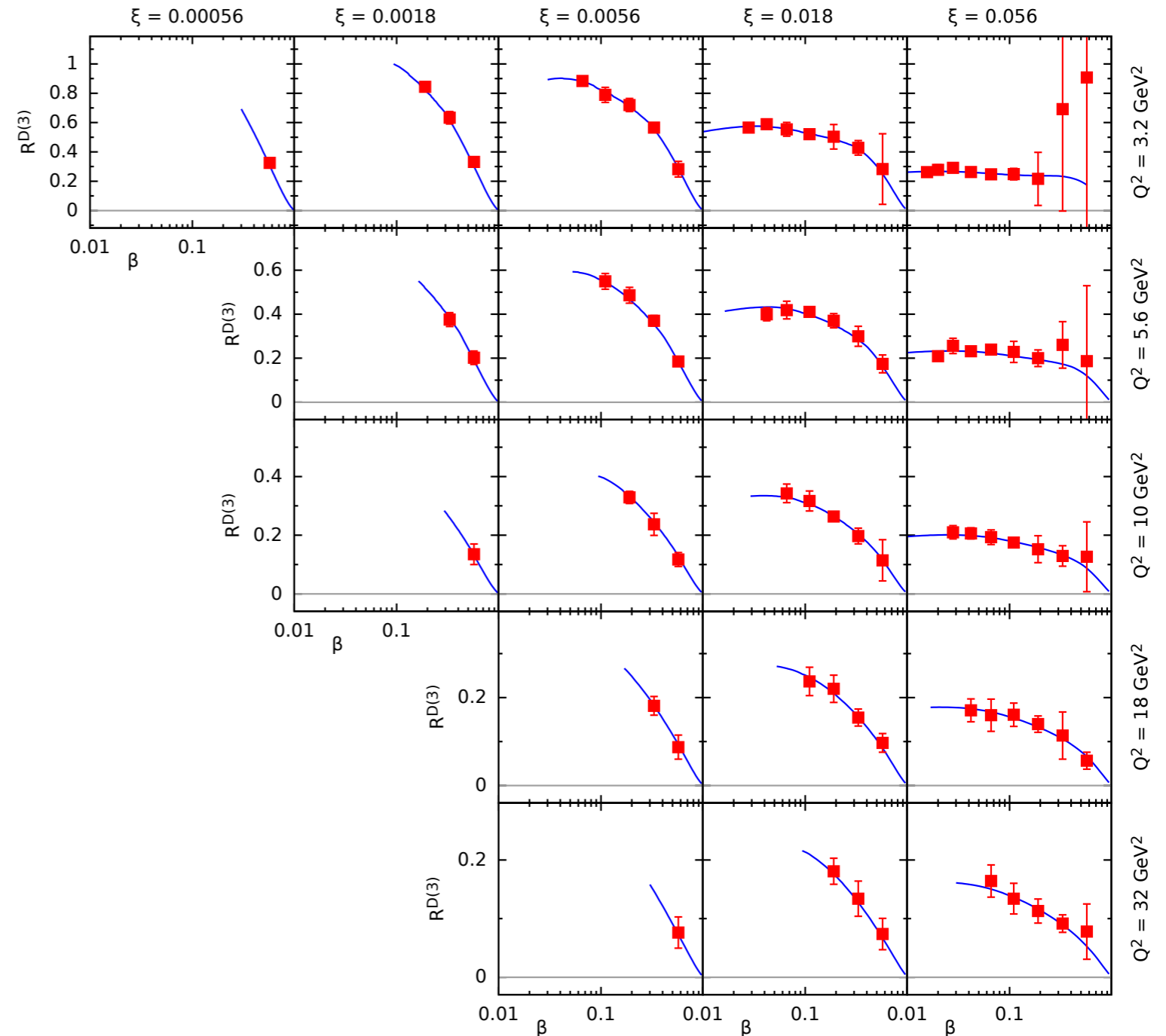
$$\sigma_{\text{red}}^{D(3)} = [1 + (1 - Y_L)R^{D(3)}]F_T^{D(3)}$$

Different form of reduced cross section

Alternative fit has different sensitivities to the uncertainties

Systematics 1%

Averaged over 10 MC samples:
reduced fluctuations



Summary on F_L^D

- $F_L^{D(3)}$ at EIC
 - Important quantity, sensitive to diffractive gluon density (saturation, higher twists...). Only one extraction at HERA by H1, large errors. Challenging measurement.
 - Three scenarios: 17, 9, 5 energy combinations. Pseudodata from DGLAP, assumed 1-2% systematics, 10 fb^{-1} integrated luminosity. Extraction via linear fit to reduced cross section
 - Scenarios S-17 and S-9 do not differ much, S-5 reduced kinematic range
 - Precision in a given bin of (Q^2, ξ, β) correlates strongly with range in inelasticity y , dominated by systematics.
 - **Good prospects for $F_L^{D(3)}$ at EIC even with 5 energy combinations**

More work:

- Other models: dipole, saturation, higher twists
- $F_L^{D(4)}$ with t -dependence. Novel analysis, never measured
- Inclusive diffraction on nuclei

Diffraction at HERA: importance of 'Reggeon'

$\xi \sigma_r^{D(4)} \simeq \xi F_2^{D(4)}$ vs ξ for fixed $|t| = 0.25 \text{ GeV}^2$ in bins of β, Q^2

Described by two contributions:

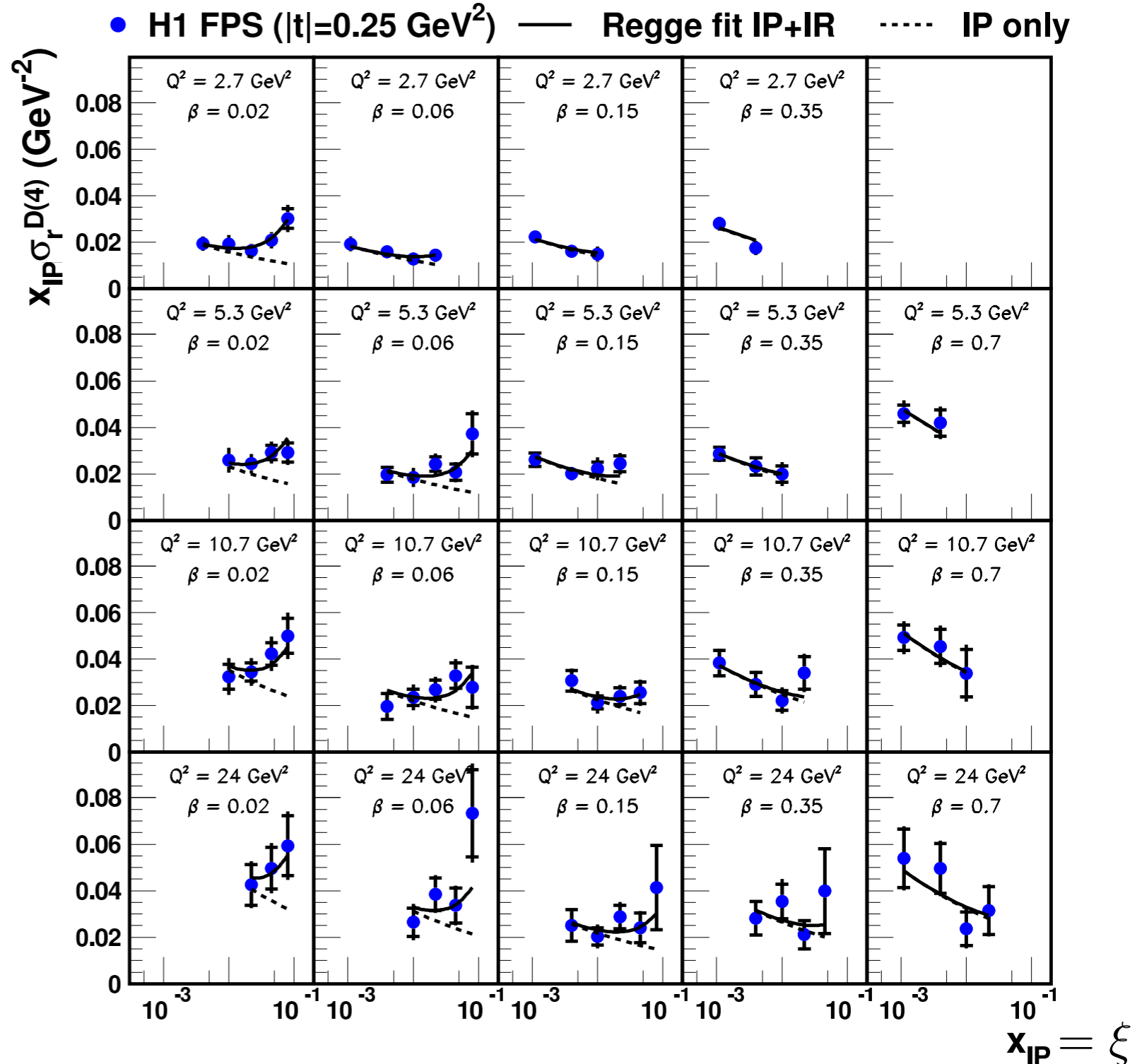
Leading 'Pomeron' at low ξ

$$\xi f_{IP} \sim \xi^{-0.22}$$

Subleading 'Reggeon' at high ξ

$$\xi f_R \sim \xi^{1.0}$$

Subleading terms poorly constrained



EIC pseudodata generation with t dependence

Use ZEUS $IP + IR$ fit with the GRV pion structure function for the IR
Pseudodata generated in all 4-variables : $(\beta = z, \xi, Q^2, t)$

Diffraction PDF:

$$f_k^{D(4)}(z, Q^2, \xi, t) = \phi_{IP}(\xi, t) f_k^{IP}(z, Q^2) + \phi_{IR}(\xi, t) f_k^{IR}(z, Q^2)$$

Fluxes:

$$\phi_M(\xi, t) = \frac{e^{B_M t}}{\xi^{2\alpha_M(t)-1}}$$

Trajectories:

$$\alpha_M(t) = \alpha_M(0) + \alpha'_M t \quad M = IP, IR$$

Reduced cross section:

$$\sigma_{\text{red}}^{D(4)} = \phi_{IP}(\xi, t) \mathcal{F}_2^{IP}(\beta, Q^2) + \phi_{IR}(\xi, t) \mathcal{F}_2^{IR}(\beta, Q^2) \\ - \frac{y^2}{Y_+} [\phi_{IP}(\xi, t) \mathcal{F}_L^{IP}(\beta, Q^2) + \phi_{IR}(\xi, t) \mathcal{F}_L^{IR}(\beta, Q^2)]$$

Flux parameters:

$$\xi \phi_{IP}(\xi, t) \propto \xi^{-0.22} e^{-7|t|}$$

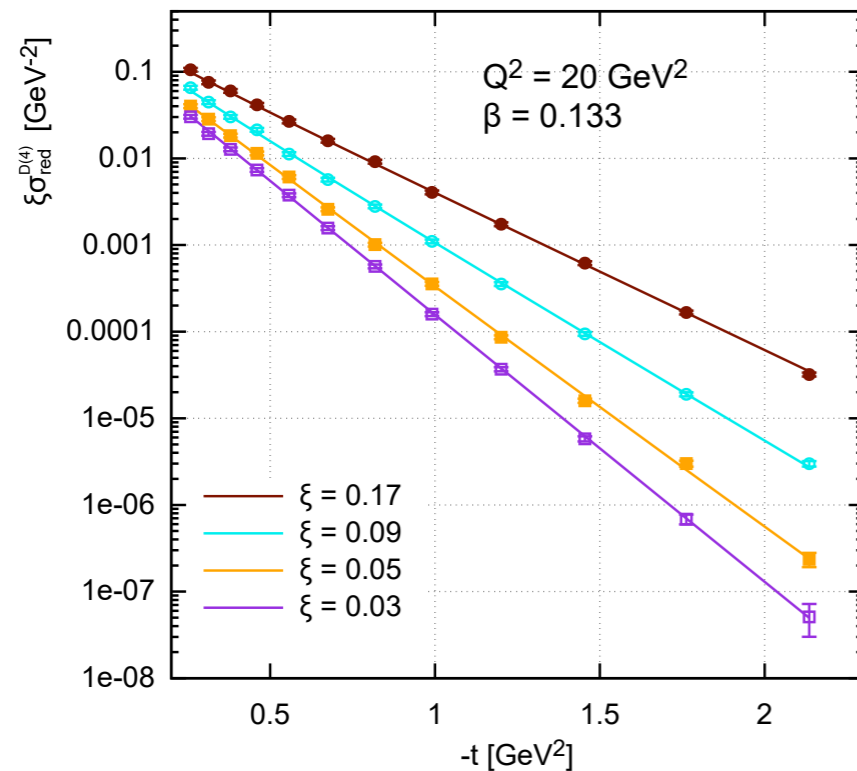
ZEUS fit
parameters

$$\xi \phi_{IR}(\xi, t) \propto \xi^{0.6+1.8|t|} e^{-2|t|} = \xi^{0.6} e^{(-2+1.8 \ln \xi) |t|}$$

EIC pseudodata generation: lumi, energy, errors

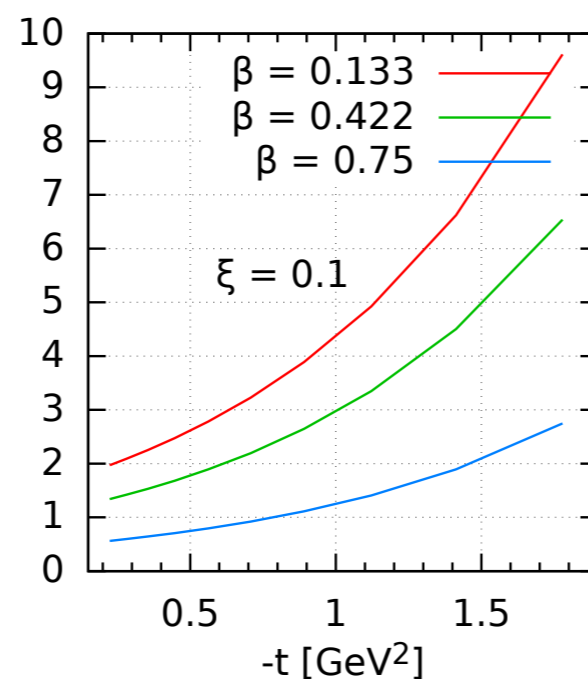
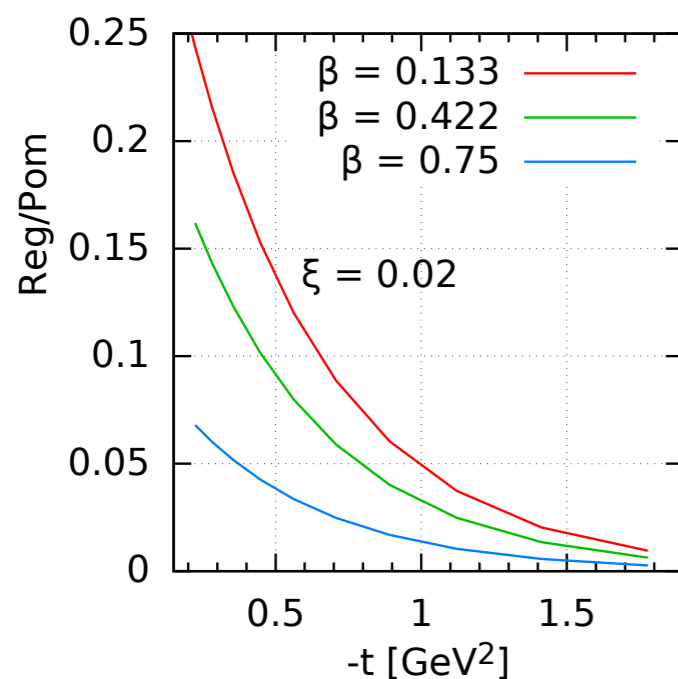
- Use NC simulations for EIC (no HERA nor CC yet)
- Three scenarios for integrated luminosity and energy :
 - $\mathcal{L} = 100 \text{ fb}^{-1}$ at high energy $E_e = 18 \text{ GeV} \times E_p = 275 \text{ GeV}$
 - $\mathcal{L} = 10 \text{ fb}^{-1}$ at high energy $E_e = 18 \text{ GeV} \times E_p = 275 \text{ GeV}$
 - $\mathcal{L} = 10 \text{ fb}^{-1}$ at low energy $E_e = 5 \text{ GeV} \times E_p = 41 \text{ GeV}$
- Require $0.005 < y < 0.96$
- Sparse and dense binning scenarios
- 5% uncorrelated systematics, 2% normalization error on top
- Randomly fluctuate each data point according to the uncertainties

Reggeon and Pomeron component in cross section at EIC



4D cross section pseudodata

- Changing t slope as transitioning from Pomeron to Reggeon dominated region
- σ_r^D slowly varying with Q^2



IR/IP ratio vs $-t$ for $\xi = 0.01, 0.1$

- Change of ratio for small vs large ξ as a function of $-t$: different slope
- $IR/IP < 1$ for small $\xi \sim 0.02$
- $IR/IP > 1$ for larger $\xi \geq 0.1$: not accessible at HERA

Parametrisation for fitting the pseudodata: full 4D fit $IP+IR$

- Treat the Pomeron and Reggeon contributions as symmetrically as possible
- Light quark separation not possible with only inclusive NC fits
- For both IP and IR fit the gluon and the sum of quarks
- Generic parametrization at $Q_0^2 = 1.8 \text{ GeV}^2$:

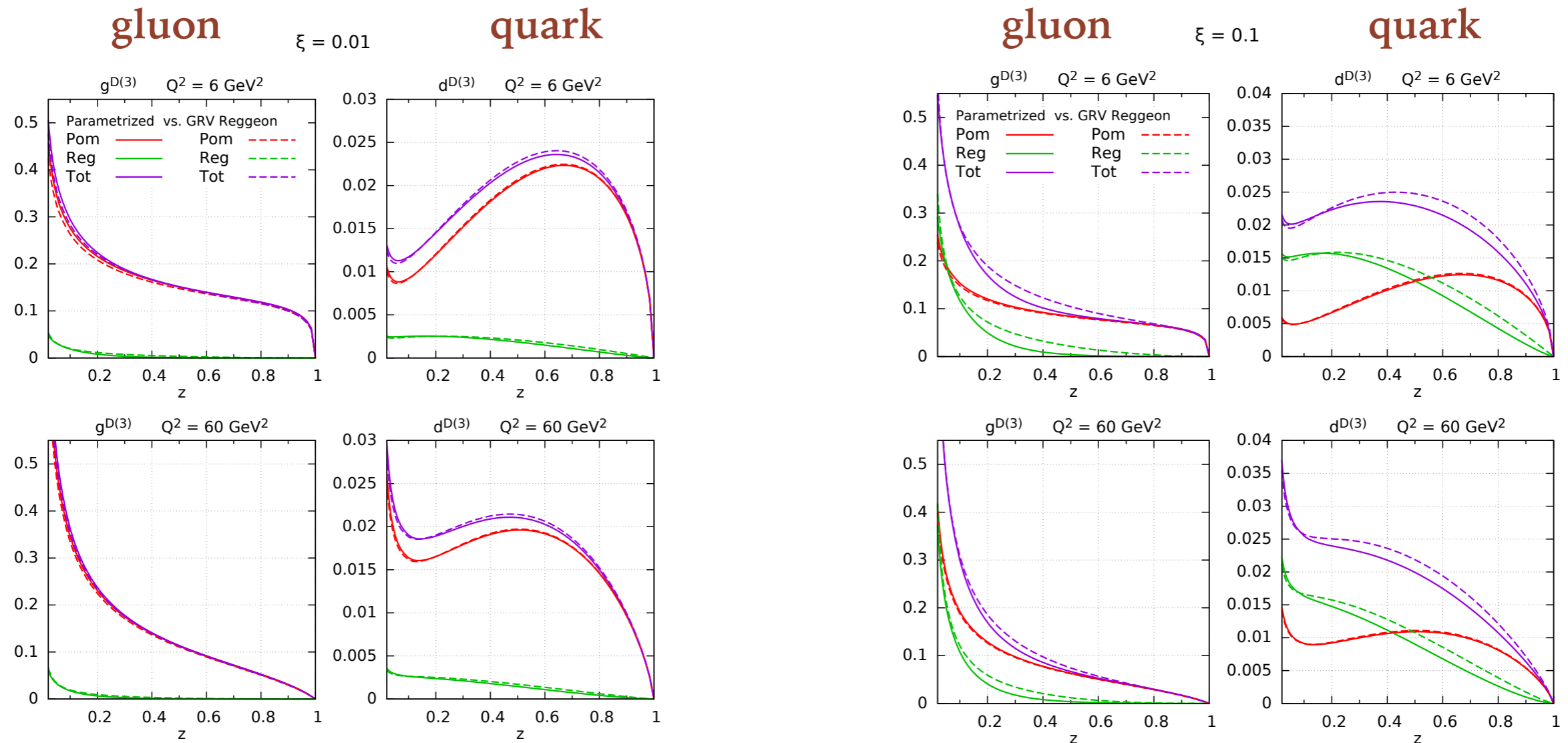
$$f_k^{(m)}(x, Q_0^2) = A_k^{(m)} x^{B_k^{(m)}} (1-x)^{C_k^{(m)}} (1 + D_k^{(m)} x^{E_k^{(m)}})$$

where $k = q, g$ and $m = IP, IR$

- Following sensitivity studies a suitable choice is:
 - f_q^{IP} has A,B,C parameters
 - f_g^{IP} has A,B,C parameters
 - f_q^{IR} has A,B,C,D parameters
 - f_g^{IR} has A,B,C parameters
- In addition fit for the parameters of the fluxes for IP and IR : $\alpha(0), \alpha', B$

$$\frac{e^{B^{(m)}t}}{\xi^{2\alpha^{(m)}(t)-1}} \quad \alpha^{(m)}(t) = \alpha^{(m)}(0) + \alpha'^{(m)}t$$

Recovering the Pomeron and Reggeon inputs



Fit results with free Reggeon parametrization (solid) made to the pseudodata based on the GRV pion structure function (dashed)

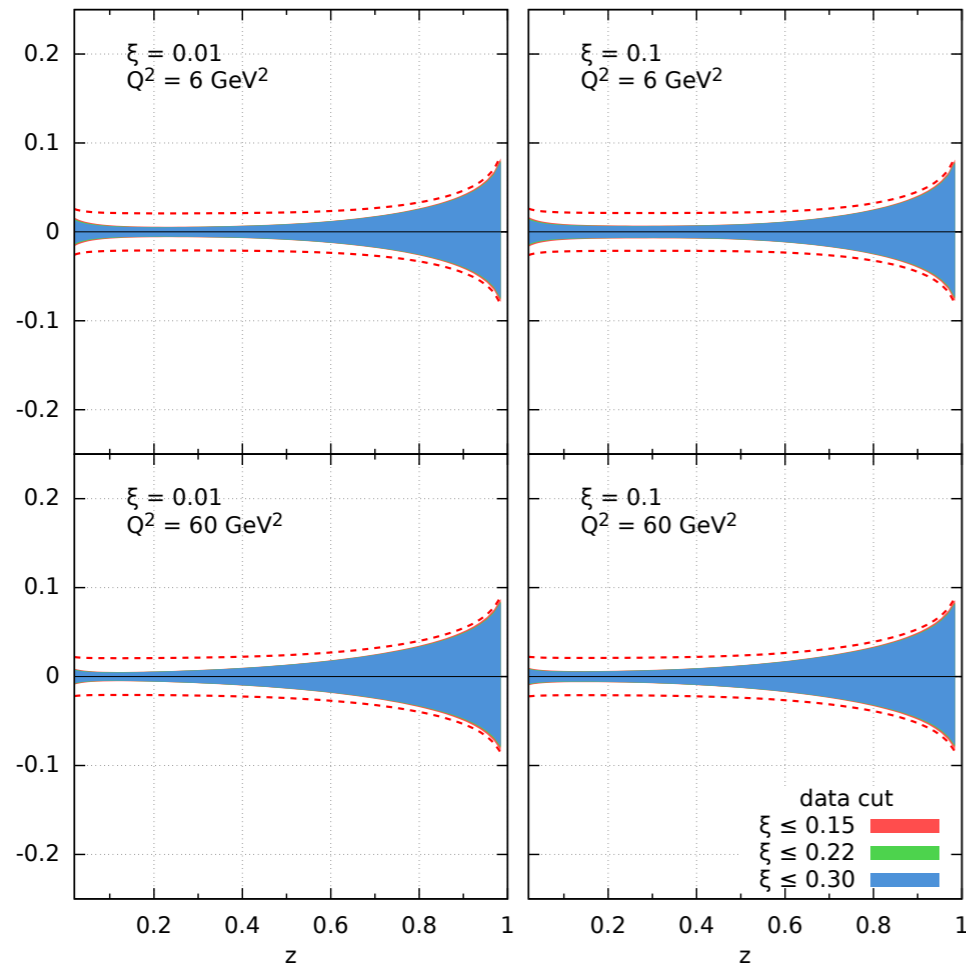
Reggeon reproduced reasonably well

Pomeron reproduced almost perfectly

Uncertainties of diffractive PDFs: Pomeron

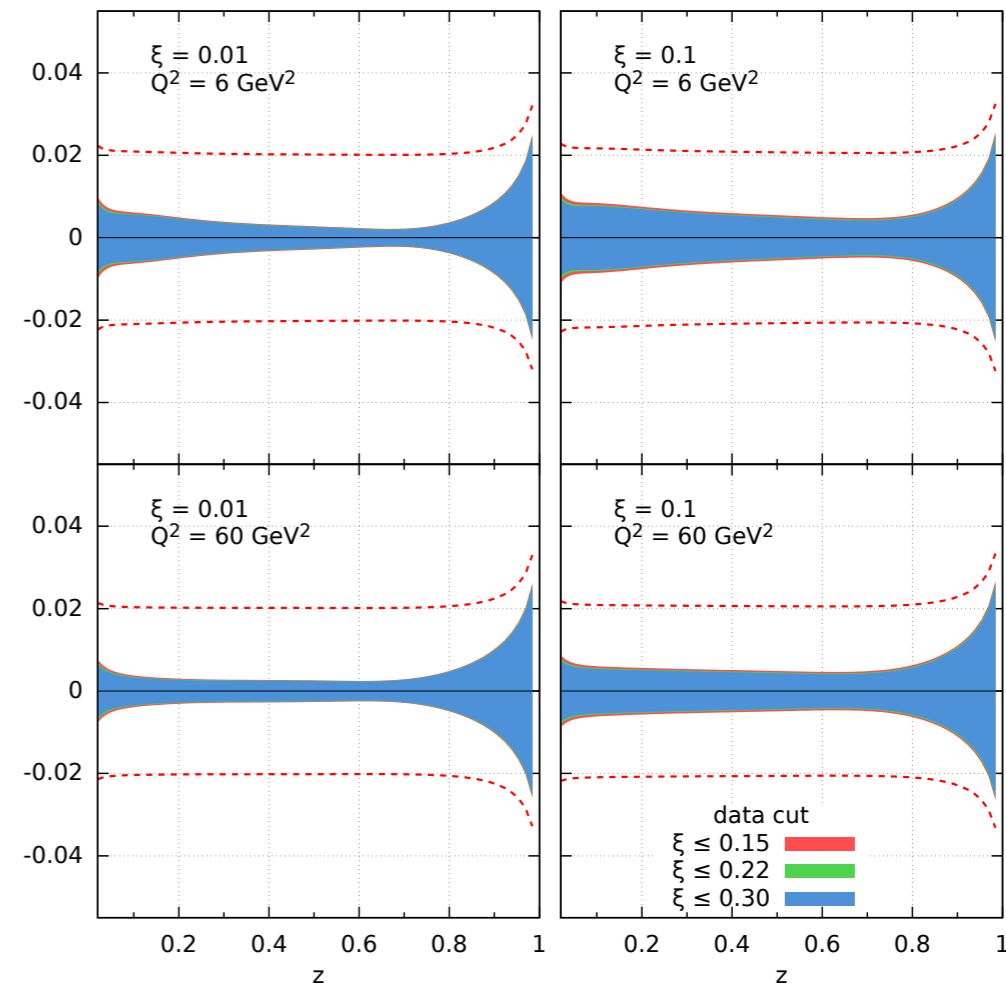
Pomeron gluon

Pomeron gluon data cut: $t \geq -1.5 \text{ GeV}^2$



Pomeron quark

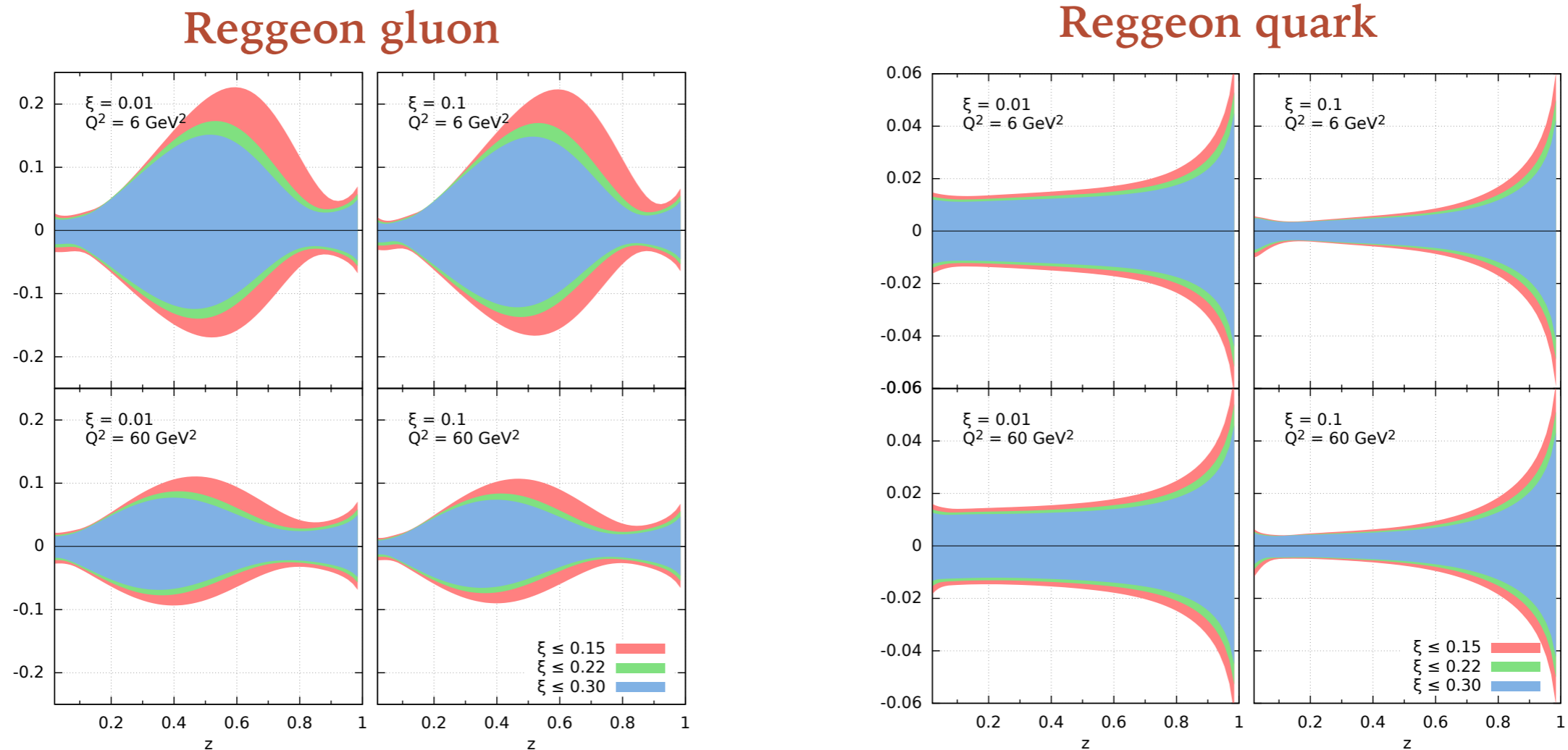
Pomeron quark data cut: $t \geq -1.5 \text{ GeV}^2$



- relative uncertainty
- <few % or better in most regions
- larger uncertainty for gluon at large z (and also small z)
- normalization error at 2% is dominant at most regions (dashed red)

*linear horizontal scale
note different vertical scale for
gluons and quarks*

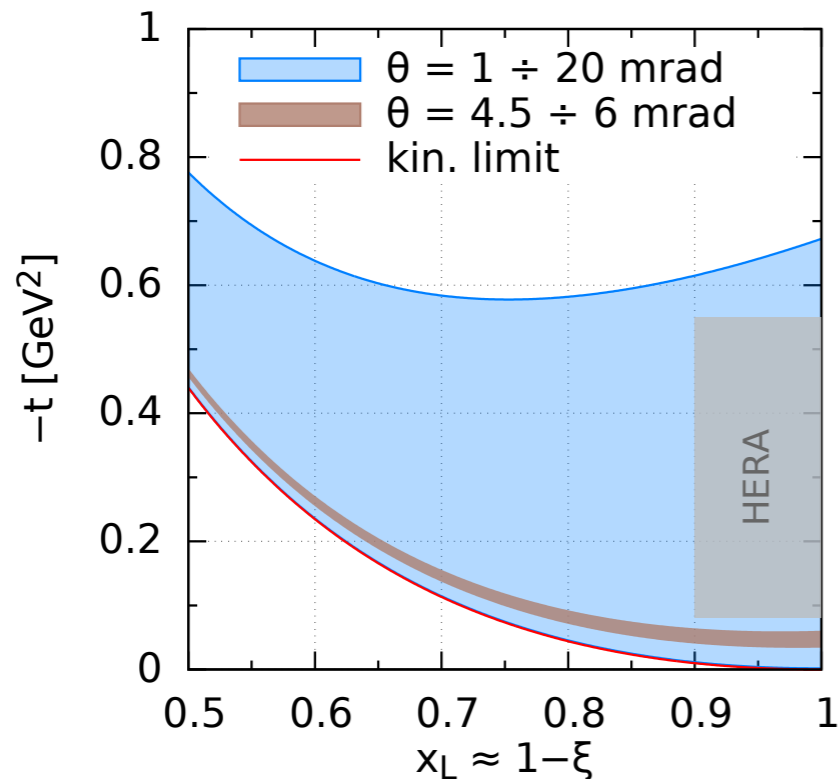
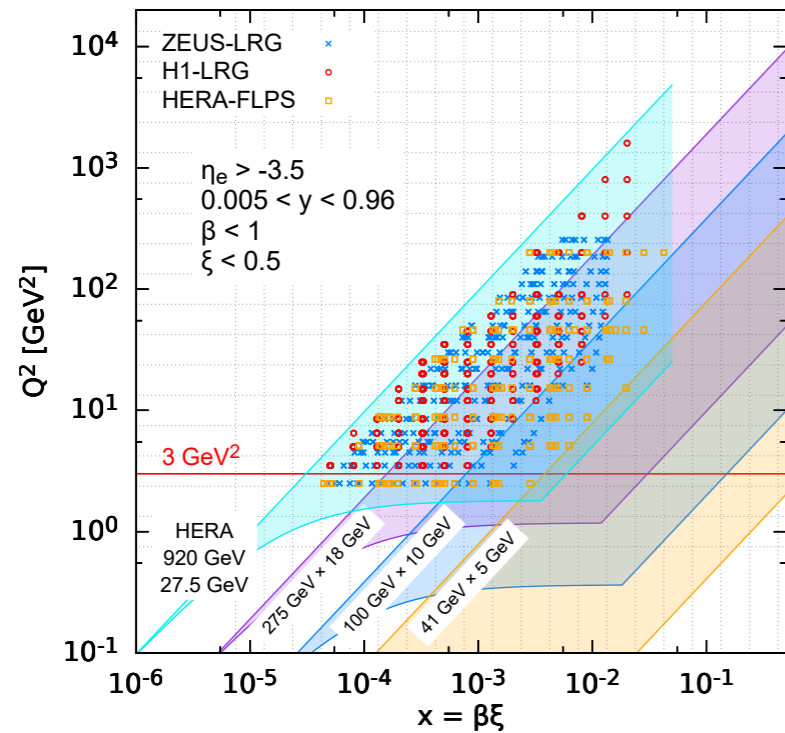
Uncertainties of diffractive PDFs: Reggeon



- $<2\%$ or better in most regions for quark except at large z
- Larger uncertainty for Reggeon gluon which is much smaller than Pomeron gluon
- Mild sensitivity to the cut on ξ for gluon, quark less sensitive
- Minimal sensitivity to the cut on t , dense vs sparse binning, lower luminosity $\mathcal{L} = 10 \text{ fb}^{-1}$

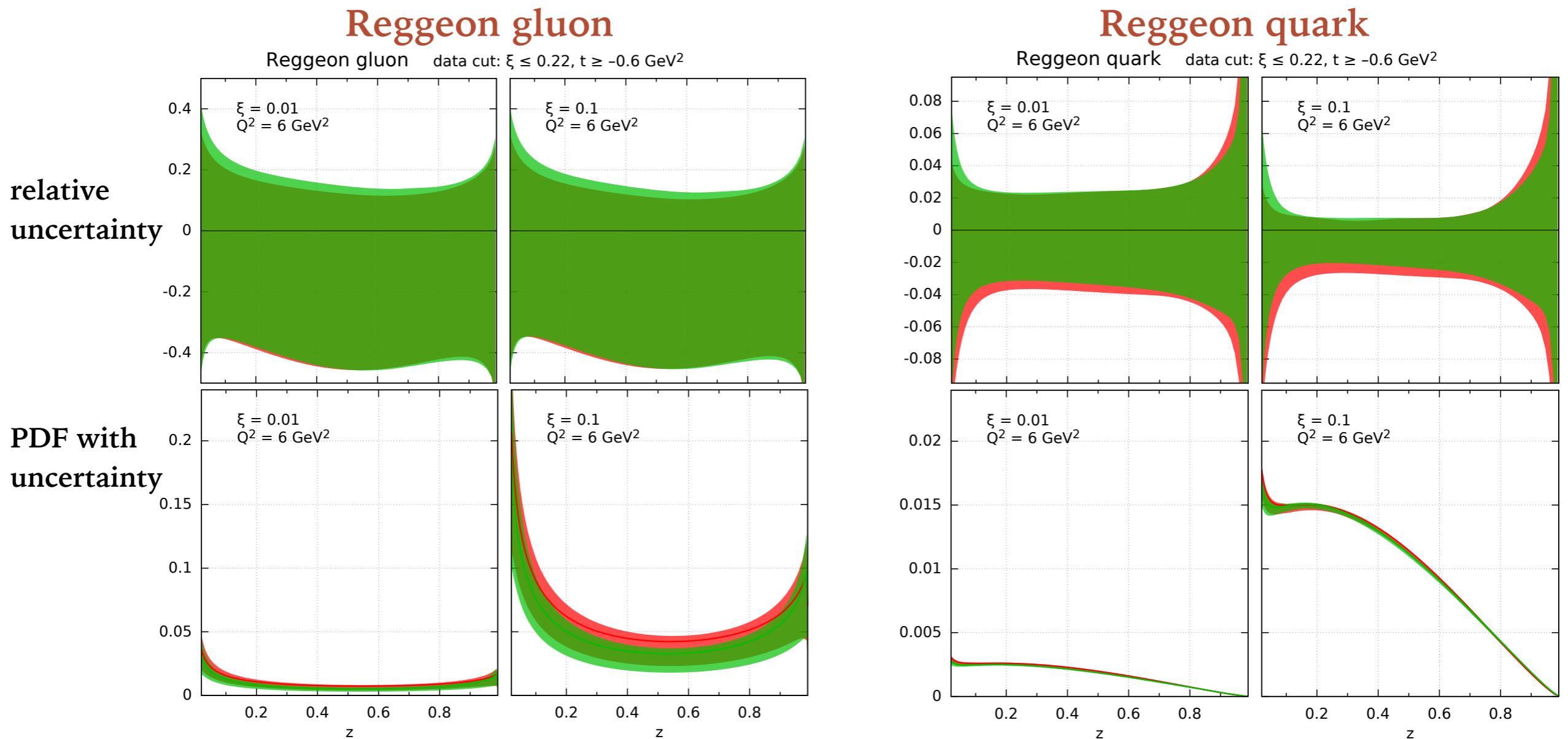
EIC can constrain Reggeon at similar level of precision as the Pomeron even when restricting data to $|t| \leq 0.5 \text{ GeV}^2$ and $\xi_{\text{max}} \simeq 0.15 \div 0.2$

Low energy scenario: 5 GeV x 41 GeV



- Low energy scenario:
 $E_e = 5 \text{ GeV} \times E_p = 41 \text{ GeV}$
- Kinematics restricted:
 - $\xi \geq 0.01$, by cms energy
 - $t \geq -0.6 \text{ GeV}^2$, forward detector acceptance
- Reggeon dominated
- Fix Pomeron from HERA and fit only Reggeon
- Luminosity $\mathcal{L} = 10 \text{ fb}^{-1}$

Low energy: Reggeon DPDFs and uncertainties



- Quark Reggeon constrained very well
- Larger uncertainty for Reggeon gluon which is much smaller than Pomeron gluon
- Two bands indicate sensitivity to two Monte Carlo samples: small variation

Low energy data at EIC can already determine Reggeon

Summary on 4D fit and Reggeon

- 4-D fit with Pomeron and Reggeon to the diffractive pseudodata
- EIC can extract flux parameters and partonic structure of the subleading ‘Reggeon’ exchange with similar precision to the leading ‘Pomeron’ exchange
- Constraints on Reggeon already from low energy run

More work needed on uncertainties:

- Experimental (correlated systematics)
- Theoretical (model dependence, parton parametrization)

Ideas for further studies:

- Combined HERA and EIC fits
- Charged current contribution